CURRENT DOT RESEARCH ON THE EFFECT OF MULTIPLE SITE DAMAGE ON STRUCTURAL INTEGRITY

P. Tong[1], K. Arin, D.Y. Jeong, R. Greif,
J.C. Brewer and S.N. Bobo
U.S. Department of Transportation
RSPA/Volpe National Transportation Systems Center
Cambridge, MA 02142

S.G. Sampath
Technical Center
Federal Aviation Administration
Atlantic City, NJ 08405

ABSTRACT

Multiple site damage (MSD) is a type of cracking that may be found in aging airplanes and which may adversely affect their continuing airworthiness. The Volpe National Transportation Systems Center has supported the Federal Aviation Administration Technical Center on structural integrity research for the past two and half years. The work has focused on understanding the behavior of MSD, detection of MSD during airframe inspection, and the avoidance of MSD in future designs. This paper addresses these three elements of the MSD problem and provides a summary of the work done, the current status, and requirements for future research.

INTRODUCTION

The occurrence of multiple site damage (MSD) in older aircraft was highlighted by the in-flight failure of a portion of the fuselage of an Aloha Airlines Boeing 737 in April 1988. The failure was precipitated by the linkup of small fatigue cracks emanating from adjacent rivet holes in the lap joint of the fuselage. Special inspections following the incident have detected MSD in aging aircraft of different makes and models. Retrospective consideration of the 1983 failure of the JAL Boeing 747 aft pressure bulkhead and the widespread cracking in the wings of the original Air Force KC-135 and C-5A suggests that MSD can occur at locations other than the fuselage. Thus, it is prudent to assume that MSD may have the potential to appear anywhere in the nation's older fleets.

This has raised concern about the continuing airworthiness of older aircraft. After the incident, the private sector and the Federal Aviation Administration (FAA) quickly went into

---

[1]Currently on leave from VNTSC as Head and Professor, Mechanical Engineering Department, Hong Kong University of Science and Technology.

action to maintain the structural integrity of older transport category airframes that are currently in service. At the International Conference on Aging Airplanes in June 1988, several interrelated technical areas were identified as key to the proper understanding of the aging airplane problem [1]. The FAA has since developed a National Aging Airplanes Research Program [2] to determine if current rules for design, inspection, and maintenance are sufficient to ensure the safe operation of the aging fleet. At the Second International Conference on Aging Airplanes in October 1989, progress of research efforts and actions taken by the FAA and the industry were reported [3]. In a subsequent meeting [4], many of the technical issues on structural integrity were addressed.

The Volpe National Transportation Systems Center (VNTSC) has supported the FAA Technical Center since February 1989 to implement the structural integrity portion of the FAA program which focuses on research to understand the behavior of MSD, techniques to find MSD during airframe inspection, and countermeasures to avoid MSD in future designs[2]. This paper addresses these three elements of the MSD problem in structural integrity research and provides a summary of accomplishments and future plans.

UNDERSTANDING MSD BEHAVIOR

As in the case of tolerance of isolated cracking, tolerance of MSD can be described in terms of detectable crack size, critical crack size, and the number of flights or flight hours of slow crack growth between these limits. All three factors can have values for MSD which are quite different from the range of values generally associated with isolated cracking. Several parallel research efforts are in progress to identify these factors for MSD.

Definition of Multiple Site Damage

Multiple site damage (MSD) is generally characterized by a group of cracks originating from similar structural details located in a common area. MSD may consist of small cracks of similar size or a large lead crack growing toward a group of small cracks. In order to define MSD more precisely, a three-part definition was proposed [7] as follows:

1. MSD is the occurrence of independent cracks which may linkup to cause greater damage or partial fracture, for which the residual strength is less than it would be if such greater damage developed as a consequence of growth of a single crack.

---

[2] The earlier progress of this work was reported in [5,6].

2. This linkup may become unstoppable due to further interaction with otherwise subcritical cracks ahead of the partial fracture.

3. A change in inspection procedure or interval from that for a single crack is needed.

Under the present definition, the occurrence of multiple cracks is not MSD if no linkup occurs or the linkup of these cracks does not result in the reduction of residual strength below the limit load which defines plastic collapse.

An example of true MSD is shown in Figures 1 and 2. The cracks are initially independent. Many can initiate and progress almost simultaneously. The linkup of these cracks may not cause catastrophic failure if the structure can sustain a two-bay skin crack at the limit load and no further cracks exist beyond the affected two bays (this would be a normally arrested fracture). However, if further cracks beyond the large one linkup to join the main fracture at low stress, the fracture may proceed uncontrollably and lead to the zipper effect. The phenomenon of cracks linking up is not specifically addressed in the current damage tolerance requirements for transport category airplanes [8,9]. Those requirements consider only the isolated cracks which constituted the airframe service fatigue experience base up to the mid-'70s.

Figure 3 shows schematically the residual strength diagram for a skin-stringer (strap or frame) combination. The structure is normally designed such that the residual strength at point A coincides with or is above the limit load. Then fracture, resulting from one of multiple cracks, will be arrested upon reaching the adjacent stiffening element because of load transfer to this element.

Now consider the MSD case of Figure 1. Its residual strength diagram is shown schematically in Figure 3 with and without MSD. The first linkups occur at relatively low stresses. Due to MSD ahead of this fracture, point A is reduced to point B in Figure 3. In other words, for stresses above point B the structure has lost its arrest capability, and the fracture can proceed at stresses below the limit load for which it was designed. Another consequence is that the critical crack length a_p is also reduced.

MSD as defined may not develop extensively in all aging aircraft. Multiple cracks might, but they are covered by damage tolerance analysis and tests. The condition for the occurrence of true MSD is the presence of sites of similar configuration subject to almost the same stress. Such cases may be few.

Chordwise stress gradients in a wingbox dictate that there will be few cracks in close proximity, which are covered by the

arrest capability at limit load. MSD is more likely in longitudinal fuselage fastener rows. At other locations, including circumferential splices, stress gradients are such that the occurrence of true MSD not covered by the damage tolerance analysis is less likely. For these configurations, a few adjacent cracks may develop. Nonetheless, after their linkup they will form a single crack which was considered in the damage tolerance analysis.

Tear Strap Effectiveness

Current design practices include the use of frame members and, in certain instances, tear straps, which act with other stiffening elements to allow the fuselage to withstand an isolated longitudinal crack up to two bays long at 110 percent of normal operating pressure plus the aerodynamic pressures in 1g flight. Fail-safety is achieved through "flapping," in which a long crack changes direction causing a controlled decompression.

One objective of the current research is to determine how effectively frames and tear straps can contain fracture in the presence of MSD. The general scenario assumes a fracture resulting from linkup of a group of MSD cracks. The fracture in this case lies along a skin splice, rather than in the mid-bay position usually assumed in present design and test practices. Also, the fracture may be advancing toward adjacent bays which contain additional (but as yet unlinked) MSD cracks.

A special fixture, which is shown in Figure 4, has been constructed to examine the residual strength and fatigue life of curved panels 68 inches on the circumference by 120 inches axially, with allowance for a range of 70 to 75 inches in radius [10].

The fixture is a shallow pressure box which accommodates the test article by means of floating seals. Hydraulically applied pressure produces hoop stress in the skin, which is reacted through lateral turnbuckles. Hydraulic cylinders and turnbuckles at the ends of the panel produce an axial stress proportional to and in phase with the hoop stress, thereby simulating the biaxial stress state found in a fuselage.

The test panels are reinforced by frames and tear straps in the circumferential direction and by stringers in the longitudinal direction as shown in Figure 5. The dimensions, construction details, and materials were chosen to replicate a configuration similar to those found in aging airplanes. The test panels do not precisely match the design of any actual aircraft model, and therefore, the test results are intended to have only generic interpretations. However, the panels will provide stress levels and structural flexibility which lie in the range of existing designs. Test results will thus be sufficiently realistic for the purposes of drawing general

conclusions about MSD behavior and calibrating damage tolerance estimation procedures.

A series of shakedown tests were performed [10] to demonstrate the successful operation of the test rig and to compare the strain fields in the panel to those calculated for a full fuselage. The initial checks were successful. The tests included five residual strength tests, where the test panels were subjected to an increasing pressure load until unstable crack growth was observed, and one fatigue test. The results of the residual strength tests are shown in Figure 6.

The effectiveness of tear straps in arresting or containing a moving crack was examined. In all of the shakedown tests involving mid-bay cracks, once instability was reached, the cracks turned at an angle of nearly 90° at the next tear strap, thereby containing or arresting the crack through flapping. Flapping, however, did not occur in the two tests involving lap splice cracks; one with and the other without MSD. That is, the lap splice cracks extended in the same direction as the crack, or in a self-similar manner. However, the early results from the second series of tests, that are presently ongoing, indicate that flapping may occur even for lap splice cracks. These most recent test results will be reported on in the future.

In the fatigue test, intentional damage was built into a panel in the form of MSD-type cracks along the upper row of rivets on the outer skin of the lap joint. In order to accelerate the crack growth process, the maximum pressure applied to the panel during cycling was 1.5 times the normal operating pressure for the last 18,300 pressurization cycles. After a total of 68,340 cycles, the panel was removed from the test fixture due to failure from cracks that had formed on the lower row of rivets on the inner skin of the lap joint. Fractographic analyses were initiated to explain this unexpected failure since the upper row, not the lower row, was notched. The results of the fractography [11] suggest that local bending amplified by the overpressure may have been the cause of the lower row failure. A striation spacing analysis of a rivet fracture surface determined that 23,500 cycles occurred between a point near one of the crack origins and a point near the switch from fatigue to ductile tearing. Another observation from the fractography is that the cracking in the tear straps occurred at the same time MSD was developing. This may further degrade the fail-safe capability of the structure.

In parallel with the curved panel test effort, analytical models have been developed to predict the failure pressure of the tests. One method of analysis, generally accepted by the aircraft industry, is the compatible displacement method [12, 13] which can readily account for the effects of rivet flexibility, biaxially applied stress, and stiffener bending. Analyses were performed assuming linear rivet flexibility (as measured in separate experiments). Comparisons between analytical and

experimental results are shown in Figure 7 for mid-bay cracks. As shown, the analytical results are dependent on the assumed value for the critical stress intensity factor. The experimental results agree well with the analytical results for K_c between 150 to 160 ksi$\sqrt{in}$. The compatible displacement analysis can be easily modified to account for the effects of nonlinear or piecewise linear rivet flexibility by implementing an iterative procedure. Figure 8 shows the analytical results from a compatible displacement analysis assuming nonlinear rivet flexibility.

Additional tests are currently being conducted that will demonstrate the residual strength of curved panels containing cracks in the lap splice. A preliminary test matrix has been developed that includes testing three (3) crack lengths with and without MSD. Also, additional fatigue tests will be conducted that will determine multiple site crack growth behavior and the effectiveness of the terminating action on curved fuselage panels.

Causes and Likelihood of MSD

To identify and counter MSD as it appears in the current fleet, and to avoid MSD in future designs, it is important to understand which design features have an increased susceptibility to develop MSD, and to predict how likely MSD is to occur in a given design.

A test program is underway to identify design features which have higher MSD potential [14]. The panels selected for fatigue tests are flat 12-inch wide panels, made from 2024-T3 clad aluminum, which contain a lap joint with three or five rows of rivets, and are reinforced along the edges to simulate stiffeners in a fuselage. A strip of aluminum is attached to the middle row of rivets to account for the local change in thickness from a stringer that is usually attached at that location on an actual aircraft. The strip has the same thickness as the crown of the stringer (nominally, 0.04 inches). A schematic of the lap joint specimens used in these tests is shown in Figure 9. The design was chosen on the basis that the panel is simple to construct and gives a stress distribution adequately representative of that in a fuselage. Figure 10 compares the stress distribution of the flat 12-inch panel with the stress fields in a fuselage as calculated by the finite element method. Additionally, MSD occurred in these panels at a life reasonably consistent with what has been observed in service for some aircraft. Figure 11 compares the crack patterns from a test on a 12 inch wide panel with those from an actual aging airplane at approximately the same number of cycles.

The test program is divided into four series. The loading in most of the tests is uniaxial tension, but some tests apply

combined tension and shear to determine the effect of mixed-mode loading on fatigue crack growth.

The first series was conducted to determine the effect of the terminating action which was mandated by the FAA for certain aging aircraft with MSD-prone lap joints. The terminating action replaces the upper-row countersink rivets with larger, button-head rivets. In particular, these tests investigate the concern that, following the terminating action, MSD may recur in the inner skin on the lower rivet row where it is difficult to detect. Referring to Figure 12, the results show that the terminating action is effective in reducing the growth rate of cracks emanating from rivet holes in the upper row of rivets.

The effect of shear loading on fatigue life of the panels was examined in the second series. These tests were conducted by applying the remote loading at an angle, thereby inducing a shear load in addition to the applied tensile load. Figure 13 shows a schematic of the load application set-up. Photographs of MSD-type cracks emanating from rivet holes at an angle of approximately 20° are evidence that a shear stress component exists in actual aircraft fuselages. For a shear-to-tension load ratio of 0.1, a reduction in fatigue life by a factor of 1.5 was observed in these tests.

The third series was designed and carried out to determine which of the following parameters have a significant influence on fatigue life and MSD formation:

Parameter	Levels Tested
a. Stress level	12, 14, and 16 ksi
b. Rivet type	flush head and Briles
c. Rivet spacing	0.75, 1.00, and 1.29 inches
d. Rivet orientation	continuous and staggered
e. Number of rivet rows	3 and 5
f. Skin Thickness	0.04, 0.05, and 0.063 inches

Three parameters with three levels and three parameters at two levels for a total of 216 ($3^3 \times 2^3$) unique combinations were possible. However, rather than establishing a baseline set of design parameters and varying each parameter one at a time, a statistical theory was used to design this experiment to reduce the number of unique test configurations while assuring that sufficient meaningful inferences could be made from the test results. A fractional factorial plan [15] was developed which reduced the number of configurations from 216 to 27; these are listed in Table 1. This experimental design also allows for evaluating the significance of pre-determined interactions. That is, the interactions of stress with rivet spacing, stress with skin thickness, and rivet spacing with skin thickness can also be evaluated for significance to fatigue life and MSD formation.

The completed data set of cycles-to-failure for all 27 configurations was analyzed by the variance method as

implemented through the Statistical Analysis Software (SAS) computer program, a commercially available software package. This program was used to test for significant differences in cycles-to-failure that could be uniquely attributable to each of the six parameters and the three interaction terms estimated from design. The results of the statistical analysis are shown in Table 2 where any parameter with a corresponding F value less than 0.05 is considered to be significant. That is, stress level, rivet type, and skin thickness have a statistically significant influence on the number of cycles to failure. Further analysis showed that the effect of stress level and rivet type is as expected; lower stress levels increase the fatigue life and the Briles rivet, which eliminates the knife edge, and also increases the fatigue life. On the other hand, the effect of skin thickness is not intuitively obvious. The preliminary analysis indicates that the greatest fatigue life is obtained with the smallest skin thickness, even though the knife edge is sharpest in this configuration. The effect of bending in the lap joint may be more significant for thicker skins.

Additional tests will be conducted to substantiate these results, and to evaluate the effect of bending on fatigue life. The statistical analysis will be repeated to determine the parameters that have a significant effect on the formation of multiple site damage.

Corrosion and Structural Integrity

Future experimental work on lap joint specimens will be conducted to determine the effect of pre-existing corrosion on fatigue initiation and crack growth behavior. A corrosion protocol will be developed that will replicate the different forms of corrosion in an accelerated manner. The ASTM standards ASTM G34 and ASTM G44 are being considered as possible candidates for the protocol. ASTM G34, also known as the "EXCO" test, is a total immersion test that replicates exfoliation corrosion by using a solution of sodium chloride, potassium nitrate, and nitric acid. ASTM G44 is an alternate immersion test that replicates pitting and intergranular corrosion, and uses a solution of sodium chloride (3.5% by weight) and water. In addition, a seacoast environment will be used as a control on these protocol experiments. Mini-lap joint specimens have been specially made of unclad 2024-T3 aluminum and will be immersed into each solution for varying times of exposure. Once an appropriate protocol has been developed, lap joint specimens will be immersed into the solution and subsequently fatigue tested. The parameters that will be varied in the fatigue testing of pre-corroded panels are: stress level, heat treatment, and degree of corrosion in terms of exposure time. Heat treatment is a variable because aluminum manufactured twenty years ago was quenched at a slower rate than aluminum manufactured today. The

tests conducted under work related to "Causes and Likelihood of MSD" will be used as the baseline for uncorroded specimens.

Improved Analysis Methods

Fracture stability analyses of stiffened flat panels have been used to correlate test data and predict damage tolerance for over two decades [12]. The models most widely used for these analyses are based on the displacement compatibility method [12,13], in which the effects of load transfer through fasteners are represented by displacement influence functions in the skins and stiffeners. Recent work has shown that the hybrid finite element method can provide excellent results more efficiently by incorporating the skin stress influence functions directly in the element [16]. The hybrid method is versatile enough to take into account the effects of complex geometry variations and different fastener configurations. It can also account for the stress singularities at crack tips and rapid stress variations near rivet holes.

The hybrid finite element method is based on a variational formulation in which relevant field variables in the element need not satisfy a priori the requirements of interelement displacement compatibility and interelement traction reciprocity. The constraint conditions can then be included in the functional by the use of Lagrange multipliers, which are the additional variables at the element boundary. The method can provide directly the solution for the strengths of singularities (such as stress intensity factors at the tips of a crack). Hybrid elements have been extensively developed and used and have been shown to be extremely accurate and efficient in comparison to the standard finite element method [16-20].

A typical problem encountered in damage tolerance analysis involves a panel with multiple cracks. As shown in Figure 14, a cracked panel is connected to stiffeners by rivets and loaded by in-plane remote stresses. The panel also is subjected to concentrated loads along rivet hole surfaces. The entire domain for the problem can be treated as a single element, commonly called a "super element".

The hybrid variational functional for the element can be written as

$$\pi_p = t[\int_{\partial A}(T_i\tilde{u}_i - \frac{1}{2}T_iu_i)\,ds + \sum_k \int_{|z-z_k|=\varepsilon}(T_i\tilde{u}_i - \frac{1}{2}T_iu_i)\,ds + \sum_k \int_{\Gamma_k}\frac{1}{2}T_iu_i\,ds - \int_{\partial A_\sigma}T_i^0\tilde{u}_i\,ds]$$

where t is the panel thickness, ∂A is the boundary of the element, $\tilde{u}_i$ are the displacements at the element boundaries. These displacements are in common with those of adjacent elements at nodal points and are piecewise polynomials along the element

boundaries. $T_i (=\sigma_{ij} v_j)$ and σ_{ij} are respectively the boundary tractions and stresses, T_i° are the prescribed tractions on ∂A_σ. The surfaces of the rivet holes are located at $|z-z_k|=\epsilon_k$, and the crack surfaces are located along Γ_k. The quantities $\tilde{u}_i$ and u_i are separate displacement fields which are independent functional variables of π_p.

The stiffness matrix for this element is then obtained by integrating over the crack surfaces and along the rivet hole surfaces. The stiffeners are modeled as beam elements. The rivets are modeled as shear springs. The energy for the beam elements and shear elements are easily expressed in the usual way. The independent variables for the problem are (i) rivet forces at rivet holes, (ii) fracture parameters representing crack singularity, (iii) stiffener deflections. The complex variable theory of elasticity is used in the formulation with Chebyshev polynomials used to represent the stresses at crack locations [20].

As a special case of the above formulation, the problem of a stiffened panel with a single crack and a broken center stiffener was analyzed. The distance between stiffeners is 12 inches and the crack length is 2a. Table 3 compares the present results (MSD) with those of the displacement compatibility method of Swift [13] and the previous finite element work of Tong [16]. Excellent agreement is seen for the correction factor ß associated with the stress intensity factor.

The mode 1 stress intensity factors for the problem involving two cracks, Figure 14, are shown in Table 4. The two central stiffeners are assumed to be broken at the crack positions, while the two outer stiffeners are intact. The distance between stiffeners is 12 inches, each crack is of length 2a and the distance between cracks is denoted by d. Table 4 shows that the stress intensity factor at the outer tip increases slowly with crack length, while that for the inner tip increases much faster as the cracks approach each other. Additional information for this problem is shown in Figure 15 for the residual strength of the structures with a panel fracture toughness of K_c = 120 ksi$\sqrt{\text{in}}$ and a stiffener ultimate strength of 82 ksi. When the crack tip is about half way to the outer intact stiffener, the stiffener residual strength is only reduced by 14.66% but the panel residual strength (based on the outer crack tip) is reduced by 72.4%.

A typical MSD situation is the lap joint shown in Figure 16, in which the cracks emanate from rivet holes in the skin. Therefore the rivet forces on the hole will have a significant contribution on the fracture parameters for the panel. To solve this problem the hybrid finite element method described earlier is used in conjunction with solutions for plates with cuts subjected to a concentrated load at the cut surface. Stress intensity factors at the crack tips can be calculated. This work is currently being developed and should prove useful in

understanding the mechanism of multiple site damage at lap joints.

The ability to model the curvature and bulging effects of fuselage panels also requires further research to make the extension to MSD. It is well established, through the results of comparative tests, that curved panels behave differently from flat panels, and that the curvature also interacts with cracks to affect properties such as damage tolerance. Flat panel models must, therefore, be empirically calibrated by comparison with curved panel tests in order to predict damage tolerance for fuselage structure. Flat panel model correction factors have been developed for the prediction of tolerance to isolated damage, but MSD correction factors have not been developed. The research approach in this case is to develop better analysis methods which account for curvature effects based on established principles of mechanics and thus require fewer validation tests than the purely empirical approach. Analysis methods are being explored or under development for determining stress intensity factors for MSD cracks in stiffened fuselage panels. The methods will account for the effects of yielding and bulging near the crack tips. These methods will be discussed in detail elsewhere in this conference.

Basic Fracture Resistance

A better understanding of basic fracture resistance properties is required in order to predict the tolerance of panels to MSD. Panel fracture predictions are currently made by means of R-curve methods, which account for the fact that a large isolated crack in a thin ductile skin can undergo stable extension at stress levels below the fracture strength. The data from which material R-curves are derived come from tests of center-cracked panels or compact tension specimens with either pin or wedge loading [21]. In all cases the specimen dimensions and length of the single crack are large if the material under test has appreciable ductility.

The results of such tests may not be applicable to damage tolerance assessments in the presence of MSD. Calculations based on the Aloha post-accident observations suggest that conventional R-curves give unconservative estimates for critical crack length. With assumptions of 1.15-inch rivet pitch and skin bypass stress corresponding to design maximum pressure, a critical crack length of 1.1 inches (tip-to-tip) is predicted from a 2024-T3 R-curve, whereas a retired 737 airframe tested by Boeing appears to suggest that the critical crack length is only 0.66 inches. Thus, a need exists to obtain coupon type data which characterizes material fracture resistance in the presence of joining details with which the MSD is associated. In fact, it is by no means clear that the R-curve approach is applicable to MSD linkup, which may be controlled by local plastic collapse (net section type failure).

As a consequence, experiments were initiated to derive special R-curves and to define the fracture resistance of panels with multiple site damage. These experiments were performed on coupons made of 2024-T3 clad aluminum sheet, 0.04 inch thick and 4 or 8 inches wide, with one row of three open holes of 0.1875-inch diameter at 1-inch pitch on center and collinear saw cuts simulating MSD [10]. Figure 17 shows a schematic of the coupon configuration. Coupons with crack lengths of 0.15, 0.22, and 0.26 inches (3.8, 5.6, and 6.6 mm) were tested. Crack growth was monitored as the coupons were subjected to increasing load until linkup. The data revealed that stable crack extension occurred even in the regime where the net section yield criterion would have predicted plastic collapse. There appeared to be no significant difference in the behavior of specimens from the as-fabricated state (blunt saw cuts) and after pre-cycling at low load to initiate a sharp fatigue crack from the central notches.

The test data seemed to suggest that the R-curve for the simulated MSD depended on initial crack length as well as extension, i.e., there was apparently no "master" curve independent of initial crack length, such as was found in conventional R-curve tests. The strain energy density criterion was used in conjunction with an elastic-plastic finite element analysis to predict the stable crack growth that was observed in these coupon tests [22]. Referring to Figure 18, reasonable, but not precise, agreement was obtained from these analyses. Differences between the experimental data and theoretical predictions can be attributed to the approximate procedure used in the elastic-plastic finite element calculations, or to the degree of accuracy in visually measuring the crack extension through a 20X microscope. Notwithstanding the lack of better agreement, these results show that the strain energy density approach provides a feasible criterion that can be used for damage tolerance evaluation of MSD-type cracks where the stability limit may be either controlled by plastic collapse or ductile fracture. An additional merit of the strain energy density criterion, not demonstrated in the present work, is its applicability to mixed mode crack growth conditions under which MSD-type cracks are commonly found.

Even if the R-curve approach is ultimately found to be inapplicable to MSD, it is still useful to have load versus crack extension data for the purpose of calibrating a plastic collapse model. However, observing crack extension through the optical microscope has thus far proved to be a difficult task because the extension increments are quite small. The raw data in most cases contains apparent jumps in crack length, a phenomenon which is believed to result from the difficulty of optically resolving small extensions and/or crack tunnelling in the specimen bulk underneath the surface cladding.

Established methods, such as optical and DC potential drop, for measuring crack length in fatigue and fracture experiments are suitable for measuring a single, identified crack of

substantial length. However, these methods do not give accurate results when applied to much smaller cracks and potential crack sites in an MSD situation.

Alternating current potential drop (ACPD) equipment and procedures have been evaluated for use in measuring small cracks typical of MSD [23]. Controlled laboratory experiments have been conducted in which the ACPD method was used to measure crack length. The test specimens were subsequently fractured, and the actual crack lengths were verified fractographically. The tests indicate that the ACPD technique can be used to measure crack growth, but that difficulties in calibrating the instrumentation may limit its practical application.

Material Behavior Characterization

A better understanding of material behavior in the presence of MSD will improve the accuracy of analysis. Both conventional and advanced fractographic techniques have been used to characterize the material behavior that can have an effect on MSD.

The fracture features of riveted lap joint specimens tested in fatigue have been analyzed fractographically [24]. The investigation included a count of fatigue striation, spacing and density, assessment of the fracture mode in the cladding near the surface, and review of the mode of failure (plane stress versus plane strain). The crack growth rates were determined from the striation spacing and reported as a function of maximum stress values. The plastic zone size was correlated with the stress intensity factor calculated for the assembly being tested.

MSD crack growth has also been investigated using an advanced quantitative fractographic technique known as FRASTA (Fracture Reconstruction Applying Surface Topographic Analysis) [25]. A three-hole specimen with crack-starter notches at the center hole was tested, first under fatigue cycling, then by applying a monotonically increasing load until the specimen failed. Analysis of the fracture surfaces produced crack profiles and fractured area projection plots for both fatigue and stable crack growth. The results revealed significant tunnelling of the crack front during the early stages of fatigue cycling, and that the crack grew at a constant opening angle during stable crack growth under monotonic loading. A finite element analysis was used to confirm the fractographic results, and to calculate the stress intensity factor and the J-Integral.

The FRASTA technique will be utilized next to compare the cracked panels taken from airplanes with those from laboratory tests of both recently made and older 2024-T3 aluminum panels. It will be applied to the fracture surfaces of fatigued panels to reconstruct the fracture events, determine microfailure mechanisms, and crack tip characteristics such as the

displacement and angle of the crack tip opening. The results are expected to indicate whether differences exist in the failure behavior of aircraft panels and panels tested under cyclic loads in the laboratory. Thus, the findings will help justify the use of laboratory test data for designing aircraft structures, setting inspection schedules, and defining maintenance procedures and may lead to improved laboratory tests that more reliably represent service conditions.

Fatigue Crack Growth in 2024-T3 Aluminum

Future work on material behavior characterization will be conducted through fatigue tests using standard specimens with 0.04-inch thickness. Particularly, the effects of stress ratio (the ratio of minimum to maximum stress), cycle frequency, strain rate, and environment will be individually explored in several series of tests.

The effect of stress ratio on fatigue crack propagation will be examined through tests performed in air. The cycling frequency will be held constant at 10 cycles per second (cps) while the stress ratio is varied. Four values will be examined: 0.05, 0.3, 0.6, and 0.8.

The effect of cycling frequency will be investigated by comparing macroscopic crack growth rates and fracture surface striation (beach marking of the fracture surface) for tests at 0.01, 10, and 20 cps. Some preliminary results indicate that the effect of frequency is negligible.

Additional tests will be conducted to determine strain rate effects on 2024-T3 alclad aluminum tensile flow stress. As part of the cycle frequency effect investigation, monotonic stress-strain relationships will be determined for strain rates varying by several orders of magnitude (0.001, 0.04, and 0.34 percent per second).

The contribution of environment to fatigue crack propagation will be evaluated by submerging crack growth specimens into aerated 3% sodium chloride (NaCl). The tests will be performed at relatively high (10 cps) and moderate (0.1 cps) frequencies. Clad and clad-removed specimens will be exposed to aerated 3% NaCl for varying lengths of time and anodic polarization voltages to establish corrosion behavior and accelerating pitted behavior.

INSPECTION FOR MSD

Proper maintenance and inspection are keys for insuring the safety of aging airframes with MSD potential. Preliminary tests and calculations suggest that MSD must be detected at quite small crack lengths and in much shorter time than an isolated crack, if MSD is to be found and repaired ahead of linkup and fracture.

The issue of inspection involves both inspection techniques and inspection interval.

Alternative Measurement Techniques

The requirements of detecting small cracks for MSD preclude reliance on visual inspection only. The only alternative which is in common usage in the airline industry involves the use of hand held eddy current probes. The eddy current method is technically reliable but tedious to apply, leading to excessive down time and human factors problems. Better nondestructive inspection (NDI) methods must be sought to provide airlines with procedures which are both appropriate for MSD and economical to apply.

New NDI technologies under consideration include infrared imaging and shearography, which have the potential to inspect a large area at a time. The capability to perform large-area inspection is especially desirable when considering the large number of rivets in a typical lap joint. Also, techniques for detecting disbonds in a lap joint are being investigated.

Under a Cooperative Research and Development Agreement between VNTSC and Henson Aviation, Inc, operator of US Air Express, a shearographic demonstration inspection (Figure 19) of some portions of a Boeing 737 aircraft fuselage was performed at a US Air repair station at Winston-Salem, NC, during August 21-23 1991. The inspection concentrated on comparing effectiveness of shearography with currently mandated methods in detecting disbonds in the fuselage.

Adhesive bonding is utilized in modern aircraft fuselages, frequently in combination with rivets. As aircraft age, bond failure becomes a major problem, since it may promote fatigue cracking, moisture intrusion, and subsequent corrosion. Any of these events may cause cabin pressure loss and, possibly, catastrophic fuselage failure.

The shearographic method of detecting disbonds depends on the deformation of the aircraft skin under varying pressurization. When illuminated by coherent light, the phase relationship and intensity of the light reflected from any two points of the skin changes as a result of this deformation. Figure 19 shows the instrument being used to inspect a lap joint for disbonds. Surface changes down to 0.00025 millimeter can be detected and displayed as a real-time image of the field of view. Comparison of successive images as the pressure changes permits interpretation of the condition of a bond.

For the portions of specific interest of the fuselage examined in this demonstration, 31 disbonds were found by shearography; 25 were confirmed by ultrasonic inspection. Of the remainder, five were disbonds on repaired riveted lap joints

where the ultrasonic device cannot perform reliably, and one was a disbond on a riveted stringer which the ultrasonic device did not detect for the same reason. In addition, there was one ultrasonic device false positive confirmed by reference to a drawing, and by observation.

The demonstration indicated potential advantages of shearography over currently used inspection techniques, specifically, potential for improved reliability in the detection of disbonds in the fuselage and reduced down-time of the aircraft while reducing inspection costs.

In a parallel activity, a library has been established which contains a variety of specimens, including pieces taken from actual airplanes as well as panels that have been used in testing. Some specimens were selected as examples of design features found in airplanes, while others display the major types of damage encountered in the aging airplane fleet, including cracks, corrosion, and disbonding. The specimens are used in calibrating NDI instruments, evaluating new techniques, and training NDI personnel.

Proof Testing

In mid-1988 a number of the independent experts who advise the FAA on structural integrity suggested that proof testing be considered as an interim backup option, to be implemented if the NDI program should prove to be ineffective, until the terminating actions specified by the Airworthiness Directives (ADs) have been applied to those airframes. The proof test is an appealing concept because it appears to eliminate the uncertainties of NDI by establishing a precise upper limit on existing crack size, relative to the critical size in flight. The proposal recommended a pressure test to limit load, i.e. 1.33 times the normal inflight pressure differential (1.33P).

The FAA/VNTSC and the National Aeronautics and Space Administration (NASA) have carried out an independent technical evaluation of the concept of pressure proof testing [26-28]. The objectives of the evaluations were to establish the potential benefit of the pressure proof test, to quantify the most desirable proof test pressure, and to quantify the required proof test interval. The focus of the evaluations was on multiple-site cracks extending from adjacent rivet holes of a typical fuselage longitudinal lap splice joint.

The FAA/VNTSC evaluation [26] involved a damage tolerance analysis of the 737 fuselage structure because of the availability of MSD crack growth data pertinent to the type of situation for which the proof test had been proposed. The effects of stress, proof pressure load, material data, rivet hole size and rivet spacing were assessed. Preliminary R-curve properties derived from the FAA/VNTSC laboratory test program

data were used to estimate the critical crack lengths corresponding to proof and maximum service pressures. A range of proof pressure was studied, not only for the effect on post-test safe crack growth interval, but also to investigate the potential for stable crack extension during the test itself. One experimental evaluation conducted under the FAA/VNTSC research program simulated the 1.33 proof factor and verified the inspection interval of the analysis.

NASA's investigation also involved a combined experimental and analytical study. Tests were conducted on panels with a long central through-crack to simulate MSD after linkup. Tests were also conducted on panels with evenly spaced unloaded holes and panels with a lap splice joint attached by a single row of rivets to simulate MSD before linkup.

The results from the two independent evaluations are summarized in Table 5 showing the required proof test interval for proof factors of 1.33 and 1.50. The proof factor is defined as the ratio of the proof test pressure load divided by the normal in-flight pressure load. The conventional factor-of-safety of 2.0 has been applied to the proof test intervals to achieve the results in Table 5. The safety factor compensates for the uncertainties involved in making crack growth life predictions.

A summary of the more general qualitative results obtained from both investigations [28] is given below.

1. The remaining life with the proof test is longer than without the proof test for a proof factor of 1.33 to 1.5.

2. The remaining life after the proof test increases with increasing proof factor up to a value about 1.5.

3. The FAA evaluation revealed that equal safety to that of proof testing could be achieved by eddy current inspection of the rivets in the splice joints at an inspection interval of about 1200 flights.

The following conclusions can be drawn from the two studies.

1. For a proof factor of 1.33, the required proof test interval must be below 300 flights to account for uncertainties in the evaluation.

2. For a proof interval of 300 flights, the proof test must be repeated on a regular basis within the period of the terminating action.

3. Conducting the proof test at a proof factor of 1.5 would considerably exceed the fuselage design limit

load and, therefore, is not consistent with accepted safe practice.

4. Better safety can be assured by implementing enhanced NDE inspection requirements and adequate reliability can be achieved by an inspection interval several times longer than the proof test interval.

As a result, pressure proof testing of the fuselage of aging commercial transport aircraft is not recommended.

Inspection Interval [7]

One key element of a successful inspection program is the interval between inspections. Too short an interval becomes economically burdensome, while too long an interval increases the possibility that a critical crack will go undetected. The selection of inspection interval (or strategy) should, therefore, be based on the required level of safety.

The cumulative probability of detection of critical cracks determines the level of safety of an inspection program. However, the decision about the required cumulative probability of detection is a difficult one. The problem becomes more apparent when it is phrased in terms of the probability that the crack will be missed. Requiring, for example, that the inspection interval be selected to provide a cumulative probability of detection of 0.98 before the crack reaches a_p, maximum permissible crack, means that it is acceptable that the crack is missed in 2% of the cases.

The conventional selection of inspection interval does not explicitly define the probability of missing a critical crack. In the conventional approach, the damage tolerance analysis is used to determine the safe crack growth period, H, which is defined as the time required for a crack subjected to a given stress spectrum to grow from the detectable to a_c, the critical size, or a_p, the permissible size. Then I=H/2 is taken as the inspection interval. This approach provides for two inspections during which a potential critical crack can be discovered and repaired. Depending on the growth characteristics and the nature of the crack, the probability of detecting the crack is different.

The above can best be illustrated by an example. Consider Figure 20, showing two crack growth curves. Assume both cracks have the same maximum permissible size a_p and H. Both will be inspected twice between a_d, detectable size, and a_p. At both inspections the case 1 crack is larger than the case 2 crack, so that the second has a higher probability of being missed than the first. For this example the crack growing fastest initially is safer by having a higher chance of being discovered.

The prediction of MSD crack growth and detection is needed in order to relate the cumulative probability of detection to different inspection intervals. A numerical model has been developed based on conventional nondestructive inspection techniques [29]. Three simple, but common, configurations were considered for illustration: (1) cracks emanating from a rivet hole; (2) crack emanating from a (large) structural hole; and (3) a corner crack in a heavy member. Crack growth was calculated using the TWIST standard spectrum [30], concurrent with the above limit load stress. Taking a case of easy access and high specificity of inspection, and taking the probability of detection (POD) curves following from a re-assessment [31-33] of the data [30], the cumulative probability of detection was calculated as a function of the length of the inspection interval, assuming visual inspection for the first two cases, and ultrasonic inspection for the third. The results are shown in Table 6.

It should be noted that this is an example only. To prevent unwarranted conclusions, the real configurations are not identified in Table 6. The cases considered were merely labelled A, B, and C, while the order is different from 1, 2, and 3 above. Table 6 shows the required inspection intervals for different cumulative probabilities of detection.

It is proposed that work be performed to obtain in-situ measurements of the POD curves for all inspection procedures used, with due account for accessibility and specificity, and to determine the cumulative probability of detection (CPOD) of critical cracks. Such information is essential to determine the associated risk of non-detection and to establish the relationship of the damage tolerance requirements (DTRs) to the safety of aging aircraft.

It is important to re-examine these DTRs so that the problems of MSD associated with aging aircraft can be avoided for the future generation of aircraft. One basis for a review of the DTRs could be a risk analysis to assess the probability of structural failures and to determine the inspection interval. This should lead to either one of the following improvements [7]:

a. Provide a definition of detectable crack size in terms of POD, if the present practice of $I = H/j$ is to be continued, and an associated definition of the safety factor j.

b. Instead of (a), require that the inspection interval be determined for a certain fixed cumulative probability of detection. This eliminates the need for a definition of the detectable crack size and for specification of a safety factor.

We shall briefly describe the risk analysis method and its required data items in the following section.

Risk Analysis

The risk analysis uses a probabilistic approach to determine the probability of failure of the single flight of a single airplane at a given time. A risk analysis [7,34] requires the following data items at the location of interest in an aircraft structure:

crack size probability distribution,
stress probability distribution,
critical crack size vs. stress,
crack growth curve, and
inspection probability of detection (POD) curve.

The POD depends heavily on the inspection method, the accessibility of the location, and the specificity of the inspection. The crack size distribution is also a function of the age of the aircraft. These data items are needed for all critical locations of the airframe in order to perform the risk analysis for the aircraft.

The crack populations at critical locations in the structure are usually difficult to obtain. Even when the data are available, they are only the data at some point in time of the service life of the aircraft. A crack growth analysis must be performed to derive the crack lengths as a function of flight hours. The crack distributions are generally obtained from destructive teardown and/or detailed inspections of the critical components.

The second required data item is the probability of exceeding a given stress at all critical locations in a single flight. This information is needed to calculate the probability of exceeding the residual strength in the flight (i.e., the probability of failure) and to predict the crack size distributions for later flights.

Crack growth prediction is normally based on fracture mechanics and is sensitive to loads (stresses and stress sequence). One way to improve the fracture analysis is to obtain more information on past loading by instrumenting aircraft to record load or stress history. The better one knows the past, the better one can anticipate the future. With the introduction of smaller and more sophisticated chips, it will become possible to equip each aircraft with a load/stress recorder. This will provide a better basis for analysis because effects such as clipping can change crack growth by factors of two and three.

The third required data item, critical crack size versus stress, is related to the residual strength of the aircraft. This information and the curve of crack growth versus flights will have to be determined by tests, a fracture analysis, or a combination of the two.

By integrating the probability of stress levels over the domain where the crack size exceeds the critical crack size for that stress, we obtain the probability of failure for the location. If the probabilities of failure of different locations are statistically independent, then the single flight probability of failure is one minus the product of the probability of no failure at all locations.

The risk assessment methodology is useful for analyzing aircraft components nearing the end of their useful lives. The single flight probability of failure provides us with an instantaneous information of the risk at some point of the aircraft's life. This interpretation of the quantity may be difficult and requires further work. Lincoln [34] suggested to relate the quantity to the risk we accept in our everyday living. For example, the risk of a major accident that we accept in driving an automobile to work and back home is of the order of 10^{-6}. Another of his suggestions is to interpret the quantity based on the precedents that have been set for other aging aircraft. He stated that, for most military systems, a single flight probability of failure of 10^{-5} or greater for an extended period of time is considered unacceptable. Whether or not these numbers are suitable for commercial transport category airplanes needs to be evaluated.

The probability of failure after a given number of flight hours should be information very valuable to airline operators and the FAA. This information is also useful for judging the effectiveness of an inspection strategy and the effect of changes in an inspection program. As of now the data required for the risk analysis of commercial transport category airplanes are not complete. The task of carrying out a rigorous risk analysis for all the airplane models is a tremendous undertaking and yet to begin.

MSD AVOIDANCE

The FAA research program not only has responded to the problems associated with MSD potential in existing fleets, but also has the objective of fostering improvement of practices to avoid MSD in the future. This goal applies to repairs as well as new designs.

A conceptual model has been developed to rank MSD potential of alternative design details [35]. The model combines fatigue and damage tolerance analyses in a practical engineering tool which yields a risk parameter. While the model is conceptually straightforward, its application requires extensive testing of realistic details subjected to realistic stress environments to provide for appropriate estimates of the fatigue life parameters.

Repair Practices

Repairs and major structural modifications often can change the MSD potential of an airframe. The general practice is to have a repair to possess static strength equal to that of the original airframe. Such a repair can become a site for later fatigue damage in the repaired or an adjacent area unless damage tolerance is also considered in the repair design.

Airframe structures which are damaged are often repaired by riveting a doubler over the damaged area. The rivets provide a load path mechanism for transfer of load from the skin to the doubler. The bearing stress induced at the rivet holes, as well as the stress concentration on the holes, will degrade the fatigue life of the skin. Reduced inspectability of these rivet holes due to doubler coverage may also be a concern. Therefore, to design a damage tolerant repair, it is essential that the calculation of loads and stresses be done to sufficient detail and accuracy so that the most critical fatigue locations can be determined and the fatigue life evaluated. The hybrid finite element method is well suited to solving repair problems. The hybrid super element accurately models the stiffened cracked panel with rivet holes, while the standard finite element method provides the versatility to take into account a variety of doubler designs, such as single doublers, two-sided doublers, laminated doublers, and finger doubler configurations [19]. An alternative approach to the analysis of riveted doubler repairs is the displacement compatibility method of Swift [36], and the recent extension of this method to two-dimensions by Battelle (under contract to VNTSC) with the program "SKINFIX". Based on the results in references [19] and [36] it can be shown that the highest rivet loads occur at the first attachment row of the doubler, with the maximum load at the corner rivet, along with the maximum skin bearing stress. Skin fatigue life can be estimated from open hole S-N data, suitably modified for stress effects using the ratio of bearing stress to gross stress. Parametric studies show the effect of doubler thickness. In general, increasing doubler thickness decreases fatigue life. Reductions in fastener load can be achieved by using multiple doublers (lamination), whether the secondary doubler is on the outside or the inside of the skin. Another technique for reducing rivet loads and consequently increasing skin fatigue life is through the use of a finger doubler configuration.

The repair of cracked structures with a bonded composite patch is a promising concept. A unidirectional composite bonded across a crack can significantly limit the crack opening and thus the stress intensity factor and crack growth. Any patch will reduce the net stress in the damaged region, but a bonded patch does not increase the number of stress concentration points (i.e., holes) as a patch fastened with rivets would. A highly orthotropic composite will not profoundly increase the transverse stiffness and thus will not significantly affect the transverse load paths. Some composite patch materials such as boron/epoxy

can provide protection against corrosion while not disrupting some nondestructive inspection (NDI) methods such as eddy current monitoring.

Analytical tools are being developed to quantify some of the benefits of composite patches [37]. Analyses show the reduction in stress intensity at the crack tip as a result of patch parameters. For example, the patch geometry shown in Figure 21 leads to the reductions in stress intensity factors shown in Figure 22. Crack geometries examined include center cracks, edge cracks, surface cracks, through cracks at the edge of loaded holes, and surface cracks at the edge of loaded holes. The lower stress intensity factors imply slower crack growth rates in these cases. This inhibited growth has been verified experimentally for some of these geometries, with specimen lives increasing by factors of up to 22. A patch has also been designed for a simulated typical lap joint with multiple site damage and has shown life improvements. This implies that composite patches may be a viable solution.

CONCLUDING REMARKS

The research progress to date and future plans are summarized as follows:

Understanding MSD Behavior

We have proposed a three-part definition to more precisely define MSD. We have also constructed a special fixture and tested the residual strength and fatigue life of cracked full scale curved panels 68 inches on the circumference by 120 inches axially. Additional tests are being conducted to demonstrate the residual strength of curved panels with and without MSD cracks in the lap splice. Also, additional fatigue tests will be conducted to determine multiple site crack growth behavior and the effectiveness of the terminating action on curved fuselage panels.

Preliminary tests indicated that tear straps were effective in providing fail-safety for running midbay cracks without MSD by causing flapping to occur, thereby containing or arresting the cracks. However, the crack did not turn at the tear straps in the two tests involving lap splice cracks, one with and the other without MSD. That is, the lap splice cracks extended beyond the tear strap in the same direction as the running crack. In parallel with the curved panel test effort, analytical models based on the compatible displacement method have been developed to predict the failure pressure of the tests. The method can readily account for the effects of rivet flexibility, biaxially applied stress, stiffener bending, and linear and nonlinear rivet flexibility (as measured in separate experiments). Good

comparisons between analytical and experimental results have been obtained.

A fatigue test indicated that cracks could be formed on rivet holes at locations other than the upper row of rivets on the outer skin. This could be due to effects of excessive local bending at those locations. Further investigations will be made to resolve the issue. The test also showed that cracking in the tear straps occurred at the same time MSD was developing which may further degrade the fail-safe capability of the structure.

We have successfully reproduced MSD in tests using flat 12-inch coupons at a life reasonably consistent with what has been observed in service. The 12-inch panel tests also demonstrated that the terminating action mandated by the FAA is effective in reducing the growth rate of cracks in the upper row of rivet holes. Full-scale curved panel tests will be conducted to confirm these tests. The test results also showed that an added shear load could cause a reduction in fatigue life and that stress level, rivet type, and skin thickness had a significant influence on fatigue. Future experimental work will be conducted on lap joint specimens to determine the effect of pre-existing corrosion on fatigue initiation and crack growth behavior.

Improved analysis methods to predict the tolerance of airframe structures to MSD are being developed. Preliminary results indicate that both the hybrid finite element method and the alternating methods are efficient and effective in accounting for the effects of complex geometry variations and different fastener configurations. These methods can also account for stress singularities at crack tips and rapid stress variations near rivet holes. Methods to account for the effects of yielding, curvature, and bulging on MSD are currently being investigated.

Test data suggests that the R-curve for simulated MSD depends on initial crack length as well as extension, i.e., there was apparently no "master" curve independent of initial crack length, as can be found in conventional R-curve tests. The strain energy density criterion was used in conjunction with elastic-plastic finite element analysis to predict the stable crack growth observed in panels with simulated MSD [22]. The results show that the strain energy density analysis is a viable approach to damage tolerance analysis of MSD where the stability limit is controlled by plastic collapse or ductile fracture.

The fracture features of riveted lap joint specimens tested in fatigue have been analyzed fractographically [24]. The crack growth rates were determined from striation spacing and reported as a function of maximum stress values. MSD crack growth has also been investigated using an advanced quantitative fractographic technique known as FRASTA [25]. Analysis of the fracture surfaces revealed significant tunneling of the crack front during the early stages of fatigue cycling, and that the

crack grew at a constant opening angle during stable crack growth under monotonic loading. The results were confirmed by a finite element analysis. The analysis was also used to determine the stress intensity factor and the J-Integral. The FRASTA technique will be used next to compare the cracked panels from the field with both recently made and older 2024-T3 aluminum panels.

Inspection for MSD

The requirements of detecting small cracks for MSD preclude reliance on visual inspection. Alternative measurement techniques are being assessed. New NDI technologies under consideration include infrared imaging and shearography, which have the potential to inspect a large area at a time. A demonstration of shearography as a method to inspect for disbonds was performed on the fuselage of a Boeing 737. The demonstration indicated potential advantages of shearography over currently used inspection techniques, such as improved reliability in the detection of disbonds in the fuselage, reduced downtime of the aircraft, and reduced inspection costs.

A library has been established which contains a variety of specimens of different design features with the major types of damage encountered in the aging airplane fleet, including cracks, corrosion, and disbonding. The specimens are used in calibrating NDI instruments, evaluating new techniques, and training NDI personnel.

The evaluation of the concept of pressure proof testing has been completed. The results indicated the required proof test interval is too short to be practical.

A methodology based on the risk analysis has been presented showing the procedures for establishing the inspection requirements. It is proposed that work be performed to obtain in-situ measurements of the POD curves for all inspection procedures and to determine the cumulative probability of detection of critical cracks. Such information is essential to determine the associated risk of non-detection and to establish the relationship of the damage tolerance requirements to the safety of aging aircraft.

MSD Avoidance

A conceptual model has been developed to rank the MSD potential of alternative design details [35]. While the model is conceptually straightforward, it requires extensive fatigue data from samples replicating realistic structural details and loading conditions.

Repairs and major structural modifications often can change the MSD potential of an airframe. Riveted doubler repairs can

degrade the fatigue life of fuselage skin unless proper care in design detail is taken. Design of repairs to an equal or better static strength capability is not sufficient for predicting fatigue life; damage tolerance principles must be used and evaluated. Reduced inspectability due to doubler coverage is also a concern. In order to fully evaluate a repair, analytic tools which are accurate and efficient must be used. VNTSC has used three analysis techniques: hybrid finite element, one-dimensional displacement compatibility, and the two-dimensional extension. These programs have been evaluated and results compared in order to fully assess all aspects of riveted repairs.

The repair of cracked structures with a bonded composite patch is being evaluated. A composite patch bonded across a crack can significantly reduce the net stress in the damaged region. This inhibits crack growth which has been verified experimentally for some geometries, with specimen lives increasing by factors of up to 22. Some composite patch materials such as boron/epoxy can provide protection against corrosion while not disrupting some nondestructive inspection (NDI) methods such as eddy current monitoring.

The FAA research program on structural integrity has gone a long way toward understanding the behavior of and controlling MSD. Many technical issues are being actively pursued. We will continuously report the progress as the research results are available.

ACKNOWLEDGEMENTS

The preparation of this paper has required the cooperation of numerous individuals within the Department of Transportation and its contractors. T. Flournoy of the FAA Technical Center is the manager of the program plan agreement between FAATC and the Volpe National Transportation Systems Center. We are also grateful for the support of T. Swift of the FAA; R. Madigan, H. Gould, H. Weinstock, J. Canha, O. Orringer, Y. Tang, J. Gordon and B. Perlman of VNTSC; Prof. R. Pelloux of the Massachusetts Institute of Technology; and the staffs of the following contractors: Arthur D. Little, Inc.; Foster-Miller, Inc.; Battelle Memorial Institute; FractuREsearch; PRC, Inc.; Stanford Research Institute International; Knowledge Systems, Inc.; and the Aeronautical Research Laboratory (Australia).

TABLE 1. TEST CONFIGURATIONS FOR WORK RELATED TO CAUSES AND LIKELIHOOD OF MSD

Configuration No.	Stress (ksi)	Rivet Type	Rivet Spacing (in.)	Rivet Orientation[1]	Number of Rows	Skin Thickness (in.)
1	12	Flush	1.00	S	5	0.040
2	12	Briles	1.00	S	3	0.050
3	12	Flush	1.00	C	5	0.063
4	12	Briles	1.29	C	5	0.040
5	12	Flush	1.29	S	5	0.050
6	12	Flush	1.29	S	3	0.063
7	12	Flush	0.75	S	3	0.040
8	12	Flush	0.75	C	5	0.050
9	12	Briles	0.75	S	5	0.063
10	14	Briles	1.00	C	3	0.040
11	14	Flush	1.00	S	5	0.050
12	14	Flush	1.00	S	5	0.063
13	14	Flush	1.29	S	5	0.040
14	14	Flush	1.29	C	3	0.050
15	14	Briles	1.29	S	5	0.063
16	14	Flush	0.75	S	5	0.040
17	14	Briles	0.75	S	5	0.050
18	14	Flush	0.75	C	3	0.063
19	16	Flush	1.00	S	5	0.040
20	16	Flush	1.00	C	5	0.050
21	16	Briles	1.00	S	3	0.063
22	16	Flush	1.29	S	3	0.040
23	16	Briles	1.29	S	5	0.050
24	16	Flush	1.29	C	5	0.063
25	16	Briles	0.75	C	5	0.040
26	16	Flush	0.75	S	3	0.050
27	16	Flush	0.75	S	5	0.063

1 Rivet Orientation: S = Staggered, C = Continuous

TABLE 2. RESULTS OF STATISTICAL SIGNIFICANCE TEST

Parameter	F Level of Significance
Stress	0.0056
Rivet type	0.0069
Skin thickness	0.0179
Rivet spacing	0.1468
Rivet orientation	0.1489
Number of rows	0.1544
Interaction of stress with rivet spacing	0.3050
Interaction of Stress with skin thickness	0.7640
Interaction of rivet spacing with skin thickness	0.9437

TABLE 3. STRESS INTENSITY CORRECTION FACTOR ß for STIFFENED PANEL WITH SINGLE CRACK ($K=\beta\sigma_{11}^{\circ}\sqrt{\pi\ a}$)

a(in.)	Hybrid Element (present)	Hybrid Element (Tong'84)	Compatible Displacement (Swift)
.375	1.58	1.58	1.56
1.125	1.31	1.31	1.38
3.000	1.17	1.17	1.21
6.000	1.11	1.11	1.12
9.000	1.06	1.06	1.06
12.000	0.848	0.849	0.869
13.500	0.699	0.682	0.713
15.000	0.710	0.681	0.696
16.500	0.705	0.688	0.695

Table 4. STRESS INTENSITY FACTORS FOR STIFFENED PANEL WITH TWO CRACKS

(per unit far field stress)

		$K_I(ksi\sqrt{in})$	
a(in.)	2a/d	Outer tip	Inner tip
0.3	0.05	1.6110	1.6121
0.6	0.1	2.0018	2.0051
1.2	0.2	2.6136	2.6249
1.8	0.3	3.0622	3.0908
2.4	0.4	3.4355	3.4960
3.0	0.5	3.8019	3.9194
3.6	0.6	4.1551	4.3741
4.2	0.7	4.4977	4.9034
4.8	0.8	4.8352	5.6172
5.4	0.9	5.2538	7.0135
5.7	0.95	5.5581	8.7794
5.9	0.98	5.8346	12.6465

d = distance between crack centers = 12-in.

TABLE 5. REQUIRED PROOF TEST INTERVAL TO SCREEN CRITICAL MULTIPLE-SITE CRACKING IN RIVETED SPLICE JOINTS

Evaluation	PROOF FACTOR 1.33 (# of Flights)	1.50 (# of Flights)
NASA	275	765
FAA	200	600

TABLE 6. INSPECTION INTERVALS AND CUMULATIVE PROBABILITY OF DETECTION FOR THREE CONFIGURATIONS [7]

Configuration	Inspection interval (hrs) for cumulative probability			I=H/2	Cumulative probability
	0.95	0.98	0.99	I (hrs)	for H/2
A	3,000	2,250	2,100	3,750	0.90
B	1,250	1,000	800	1,250	0.95
C	5,700	4,500	4,000	7,500	0.89

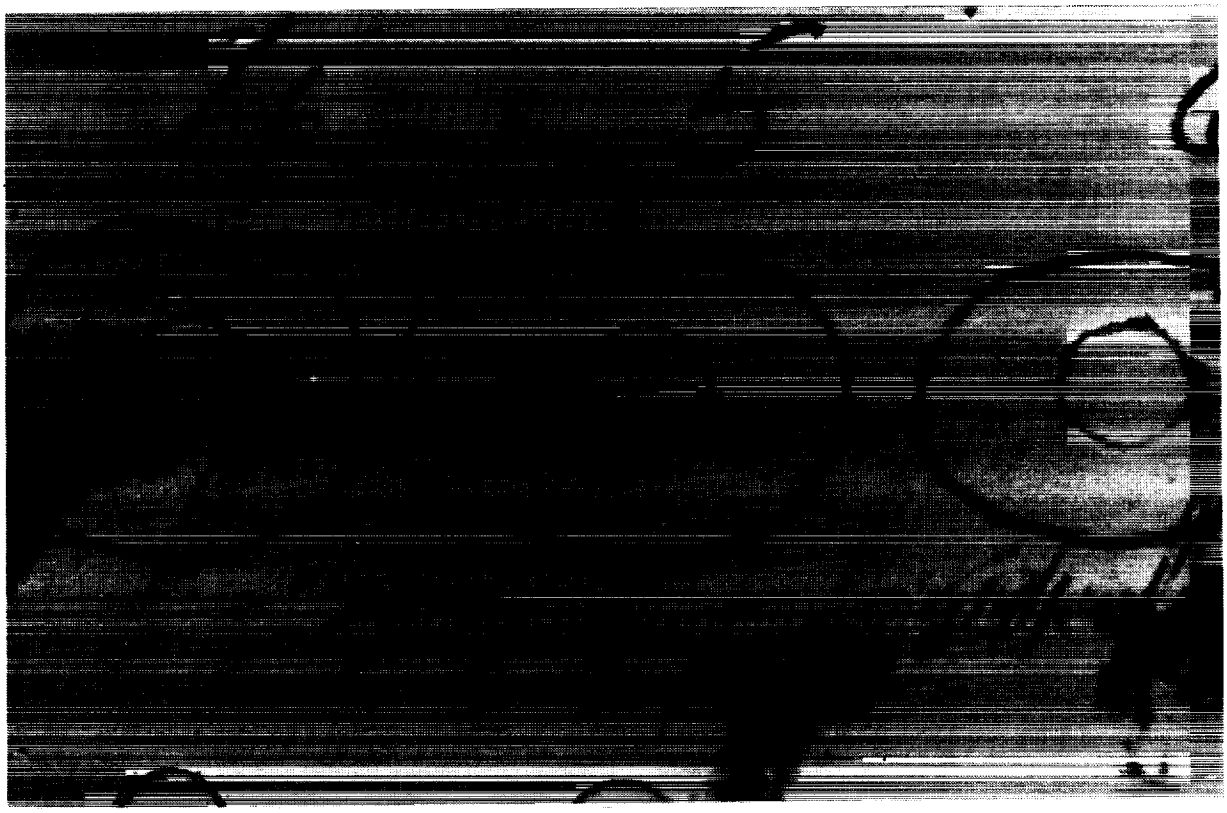

FIGURE 1. MULTIPLE SITE DAMAGE IN N73711
(FROM REFERENCE [3], COURTESY OF T. SWIFT).

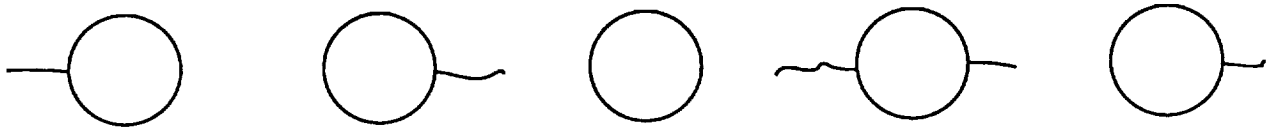

FIGURE 2. SCHEMATIC OF A TYPICAL MSD CONFIGURATION.

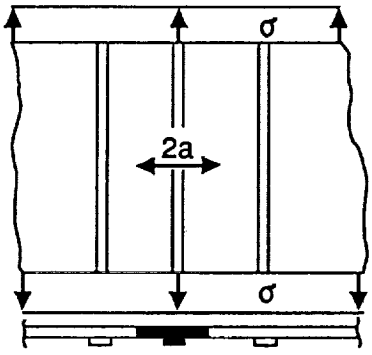

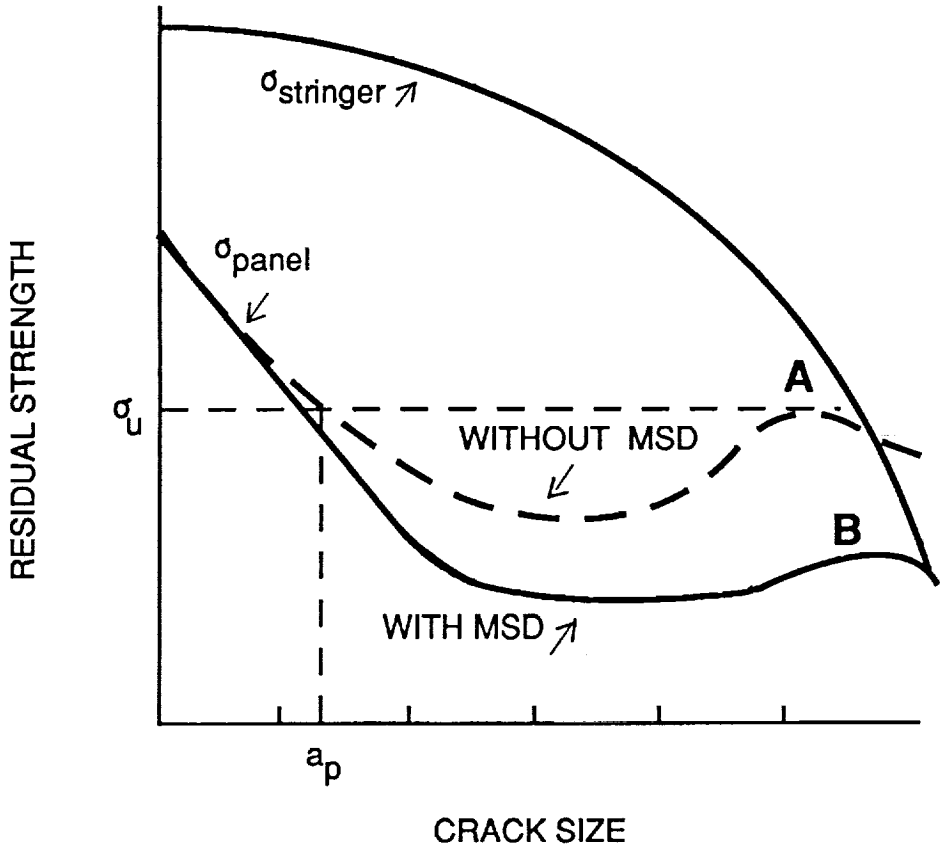

FIGURE 3. EFFECT OF MSD ON RESIDUAL STRENGTH (REFERENCE [7])

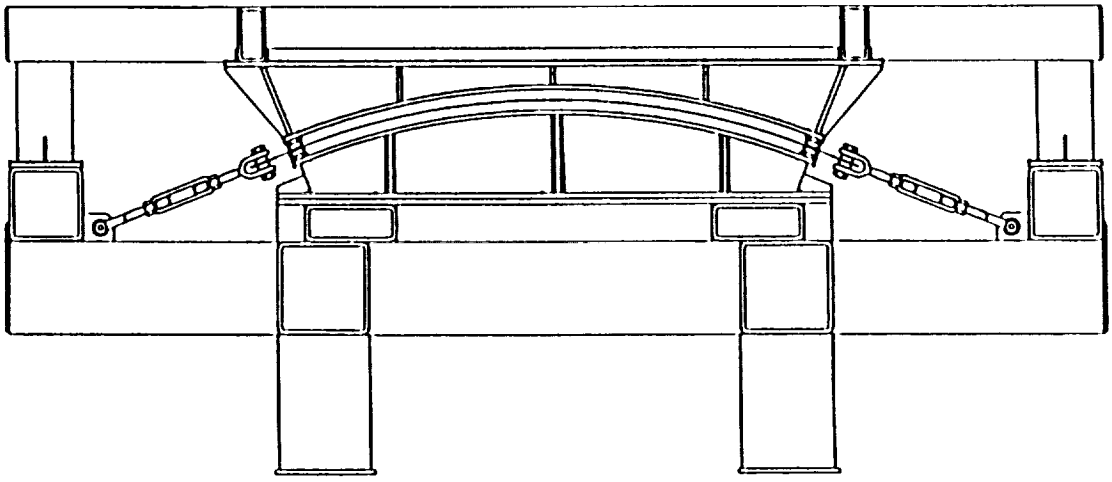

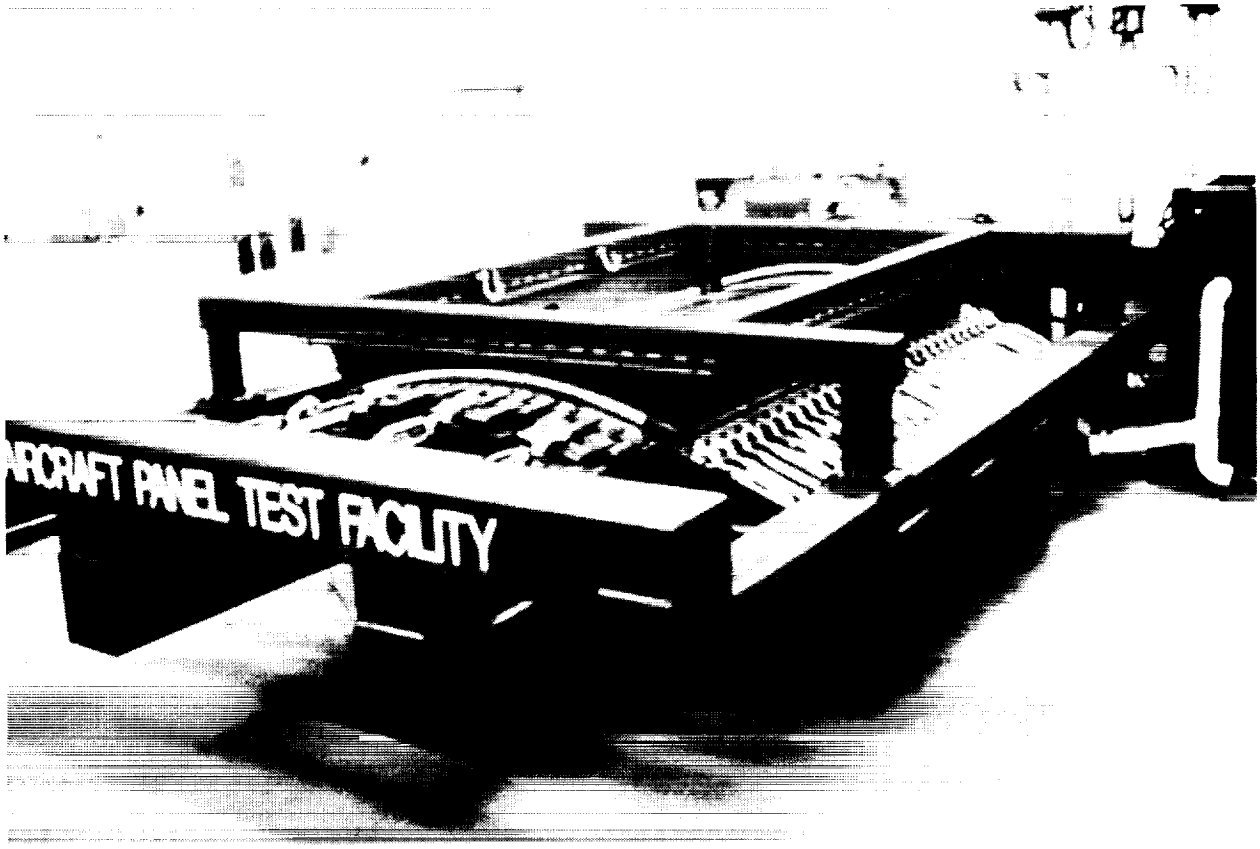

FIGURE 4. CURVED PANEL TEST FIXTURE

ORIGINAL PAGE
BLACK AND WHITE PHOTOGRAPH

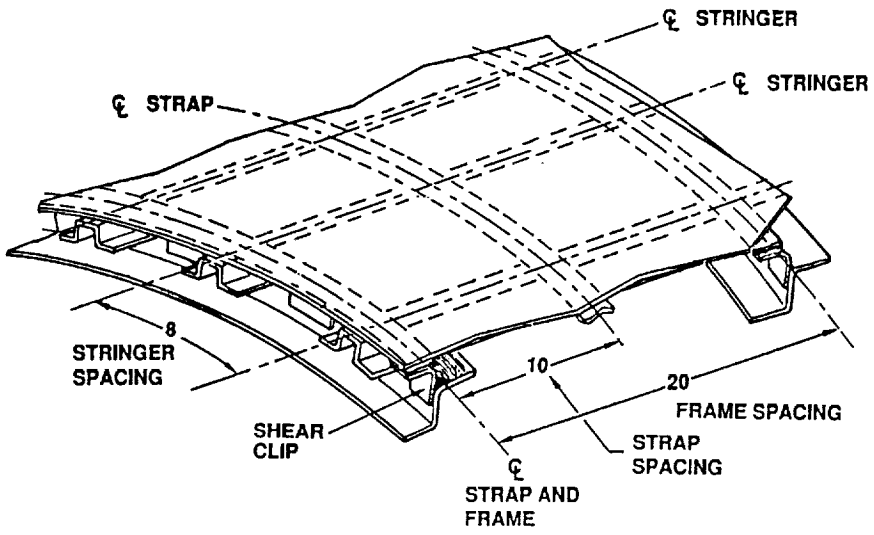

FIGURE 5. STRUCTUAL DETAILS OF CURVED TEST PANEL

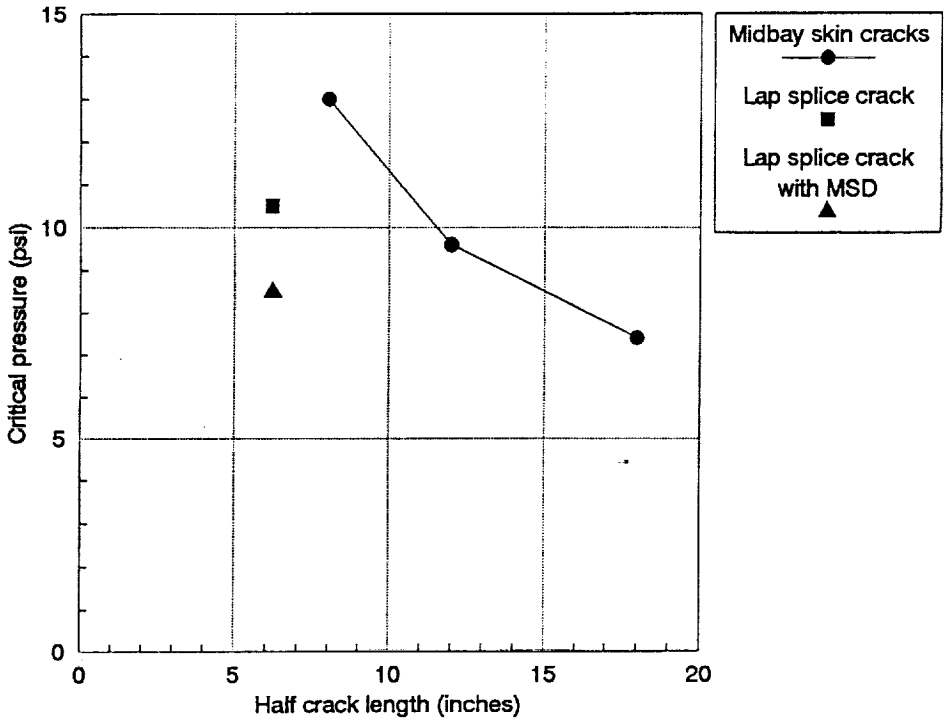

FIGURE 6. CURVED PANEL SHAKEDOWN TEST RESULTS

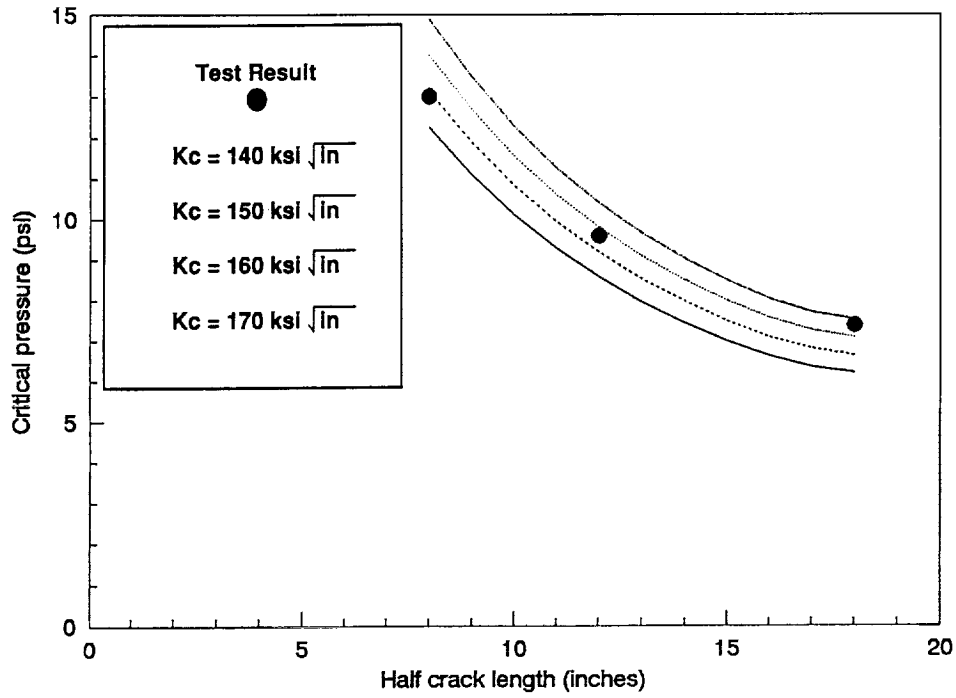

FIGURE 7. COMPARISON OF CURVED PANEL TESTS AND ANALYSIS

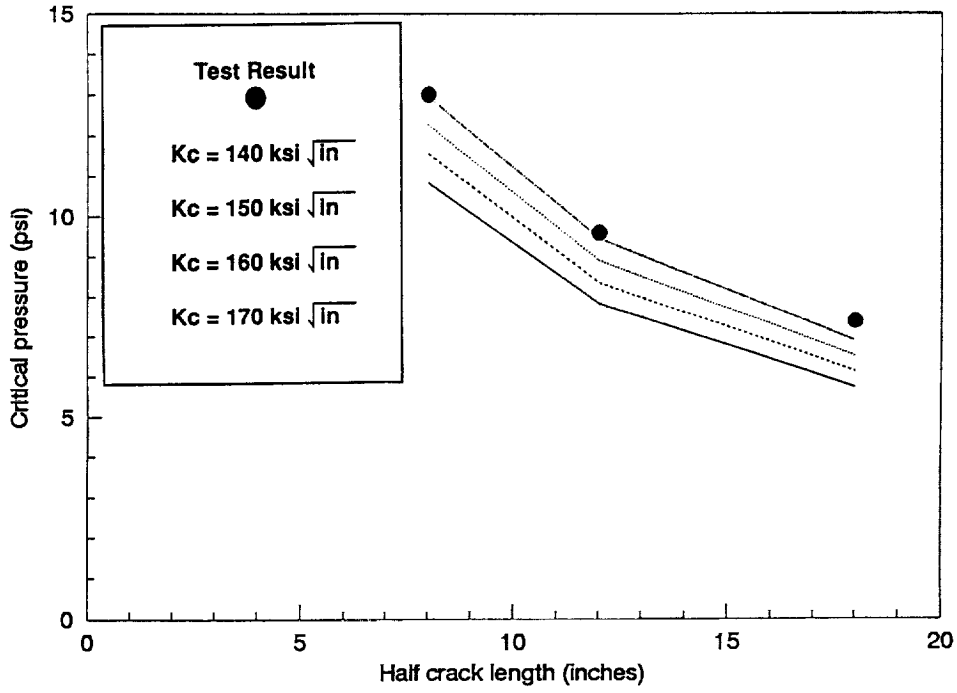

FIGURE 8. RESULTS OF ANALYSIS ASSUMING NON-LINEAR RIVET FLEXIBILITY

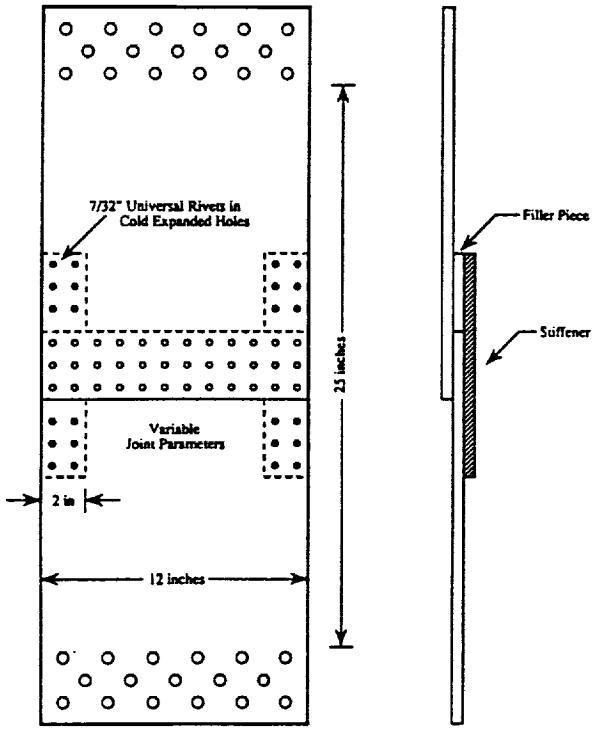

FIGURE 9. 12-INCH TEST PANEL

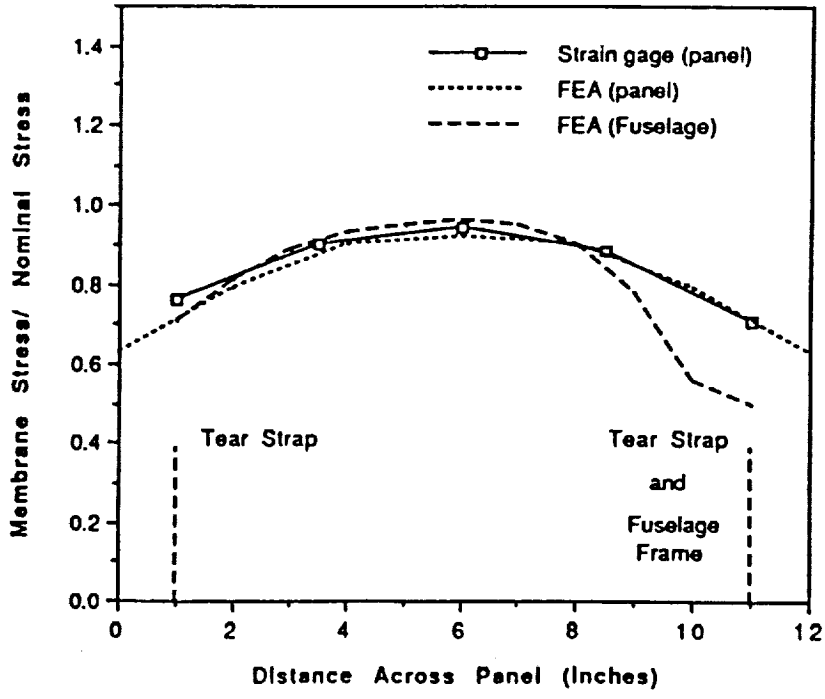

FIGURE 10. STRESS DISTRIBUTION IN 12-INCH PANEL

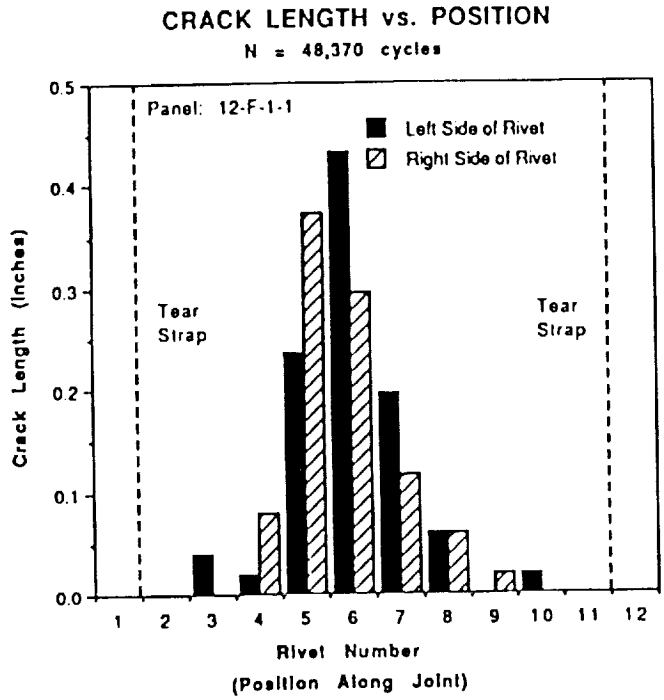

FIGURE 11A. CRACK PATTERN FROM 12-INCH PANEL TEST

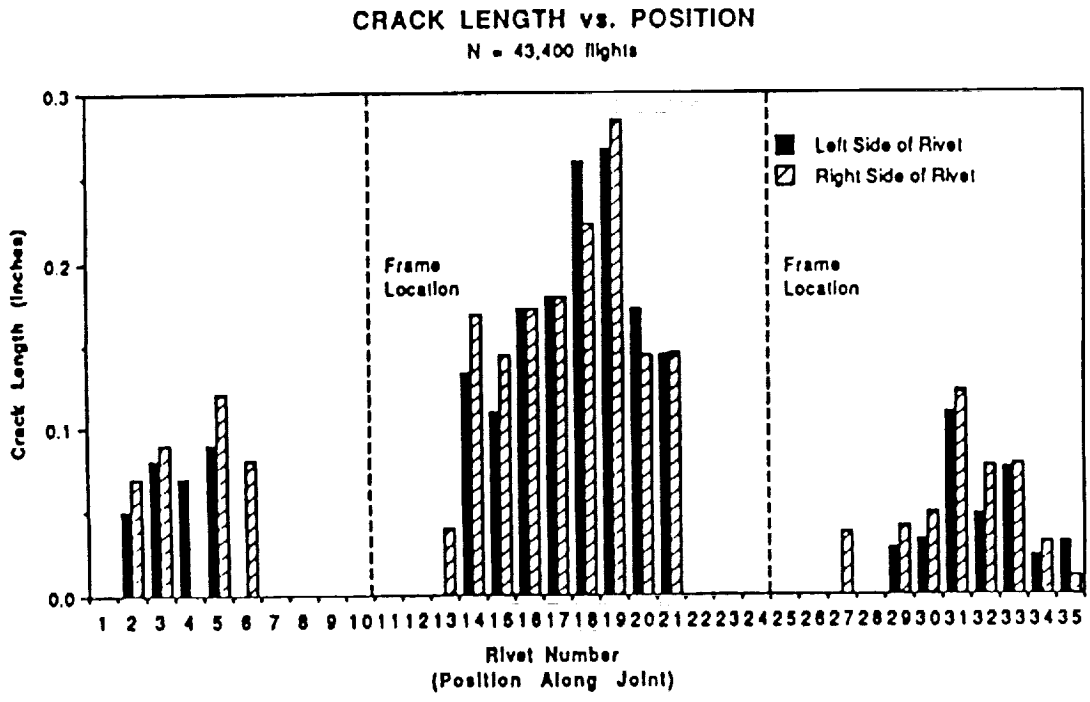

FIGURE 11B. CRACK PATTERN OBSERVED IN AN AGING AIRCRAFT

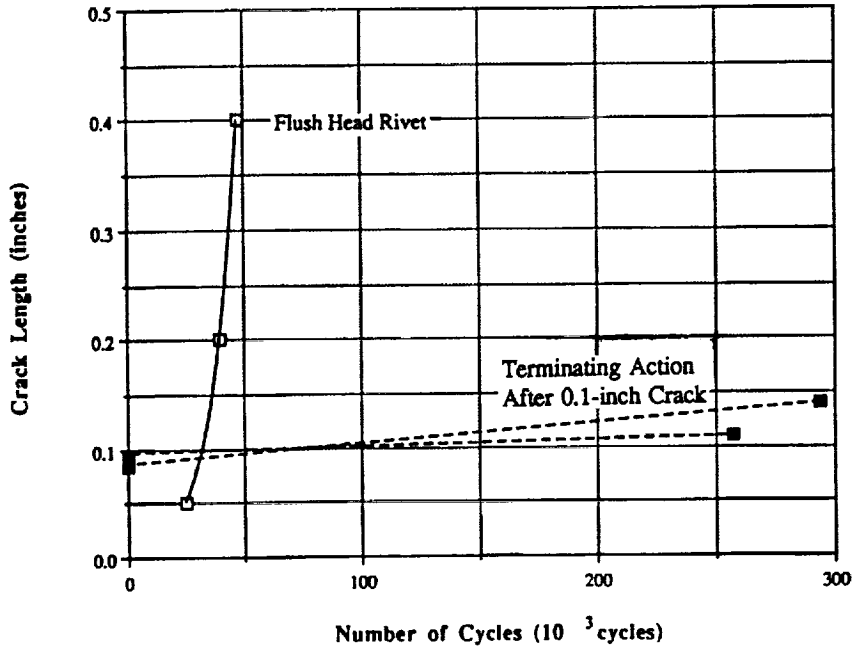

FIGURE 12. EFFECT OF TERMINATING ACTION ON CRACK GROWTH RATE

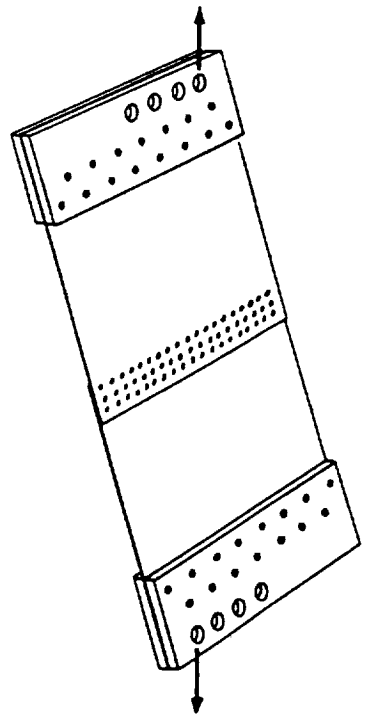

FIGURE 13. SCHEMATIC OF COMBINED SHEAR AND TENSION TEST PANEL

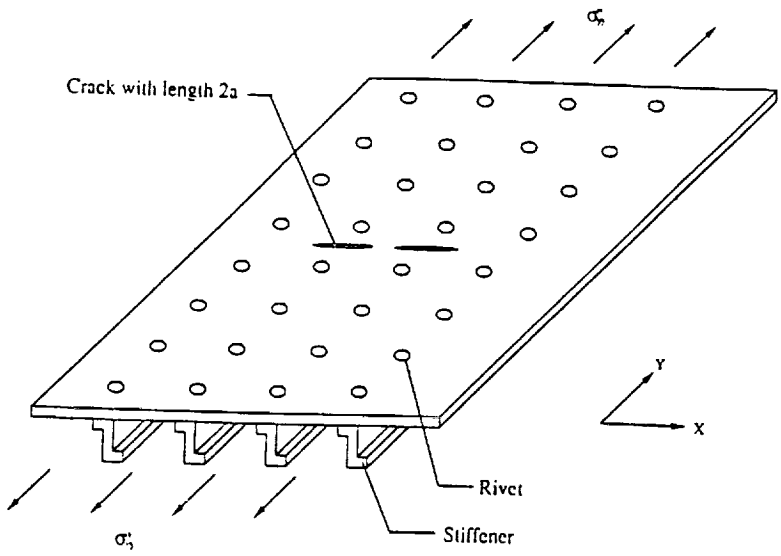

FIGURE 14. STIFFENED PANEL WITH TWO CRACKS

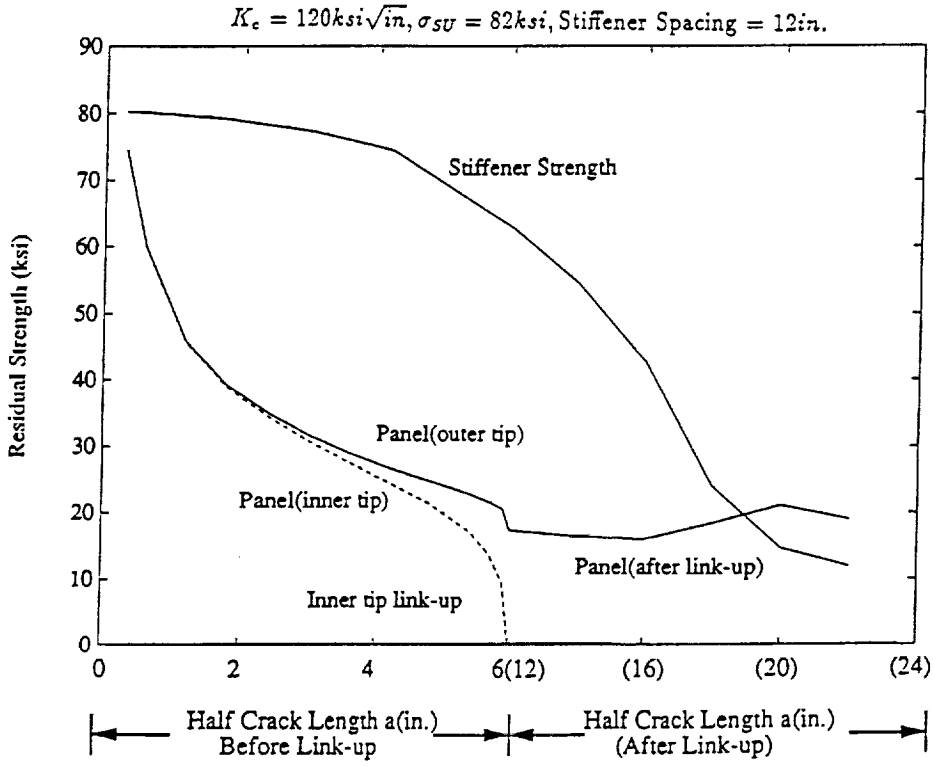

FIGURE 15. RESIDUAL STRENGTH OF THE STIFFENED PANEL

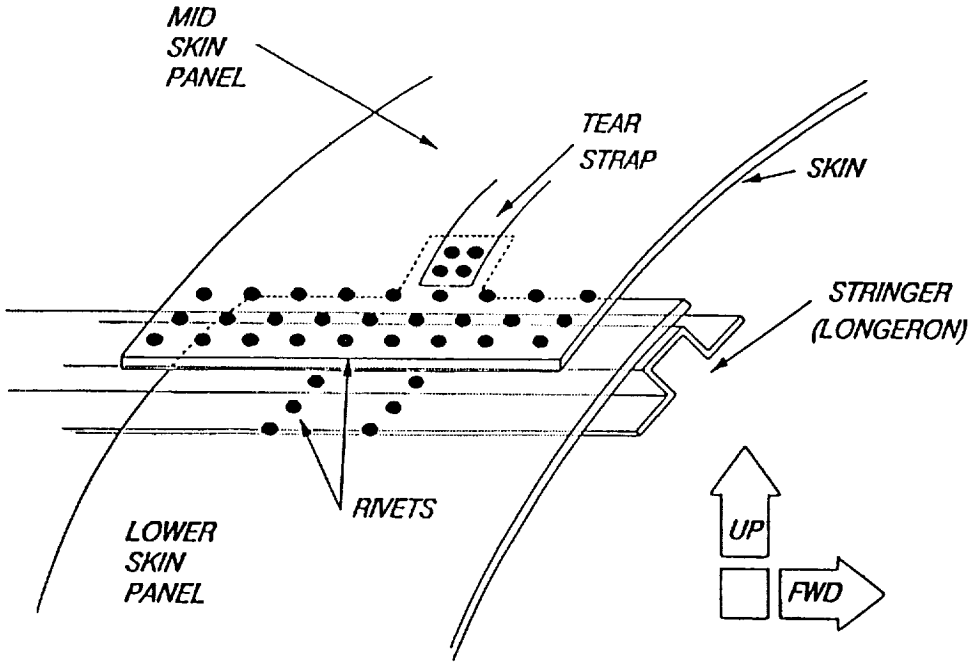

FIGURE 16. SKETCH OF TYPICAL RIVETED LAP-JOINTED FUSLEAGE PANELS (FROM REFERENCE [4])

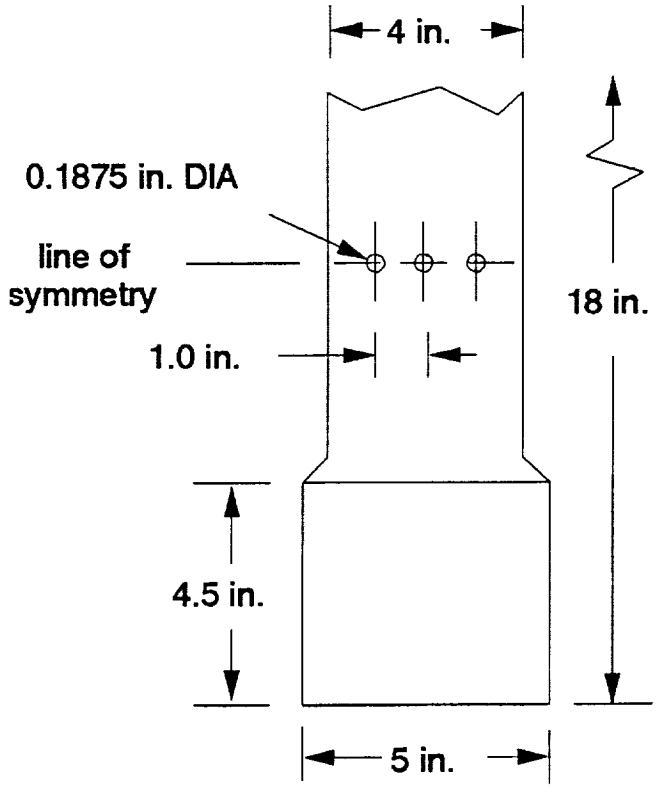

FIGURE 17. SCHEMATIC OF COUPON WITH SIMULATED MSD

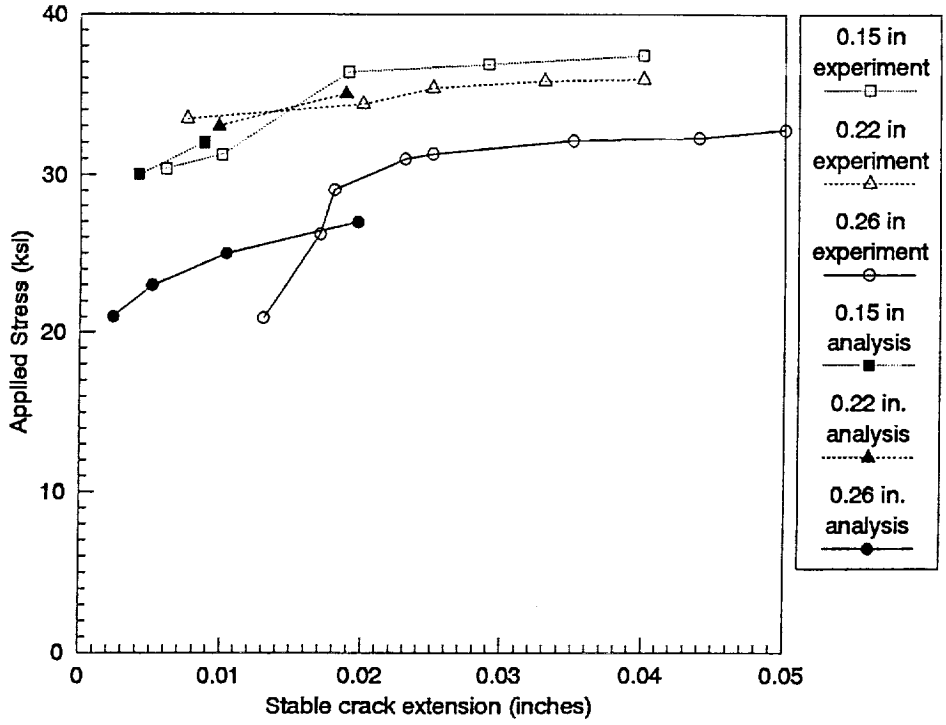

FIGURE 18. COMPARISON OF ANALYTICAL AND EXPERIMENTAL RESULTS FOR COUPONS

FIGURE 19. TRIPOD-MOUNTED SHEAROGRAPHIC INSPECTION SYSTEM

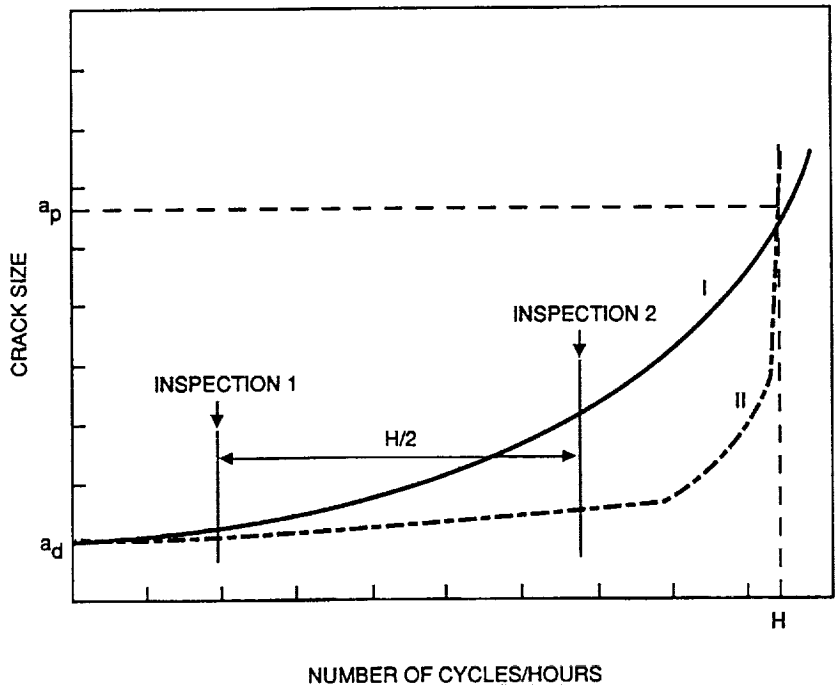

FIGURE 20. SIGNIFICANCE OF RELATION BETWEEN CRACK GROWTH AND INSPECTION INTERVAL (REFERENCE [7])

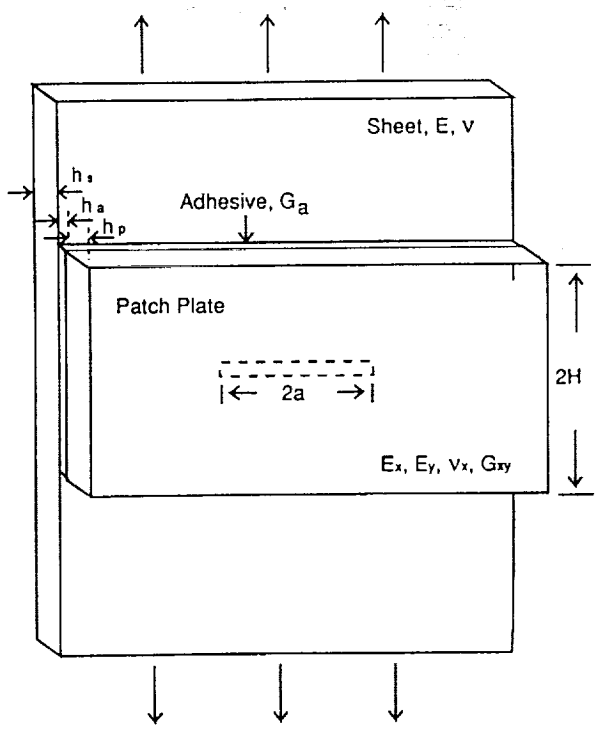

FIGURE 21. PATCH ON A CENTER-CRACKED PLATE (FROM REFERENCE [37])

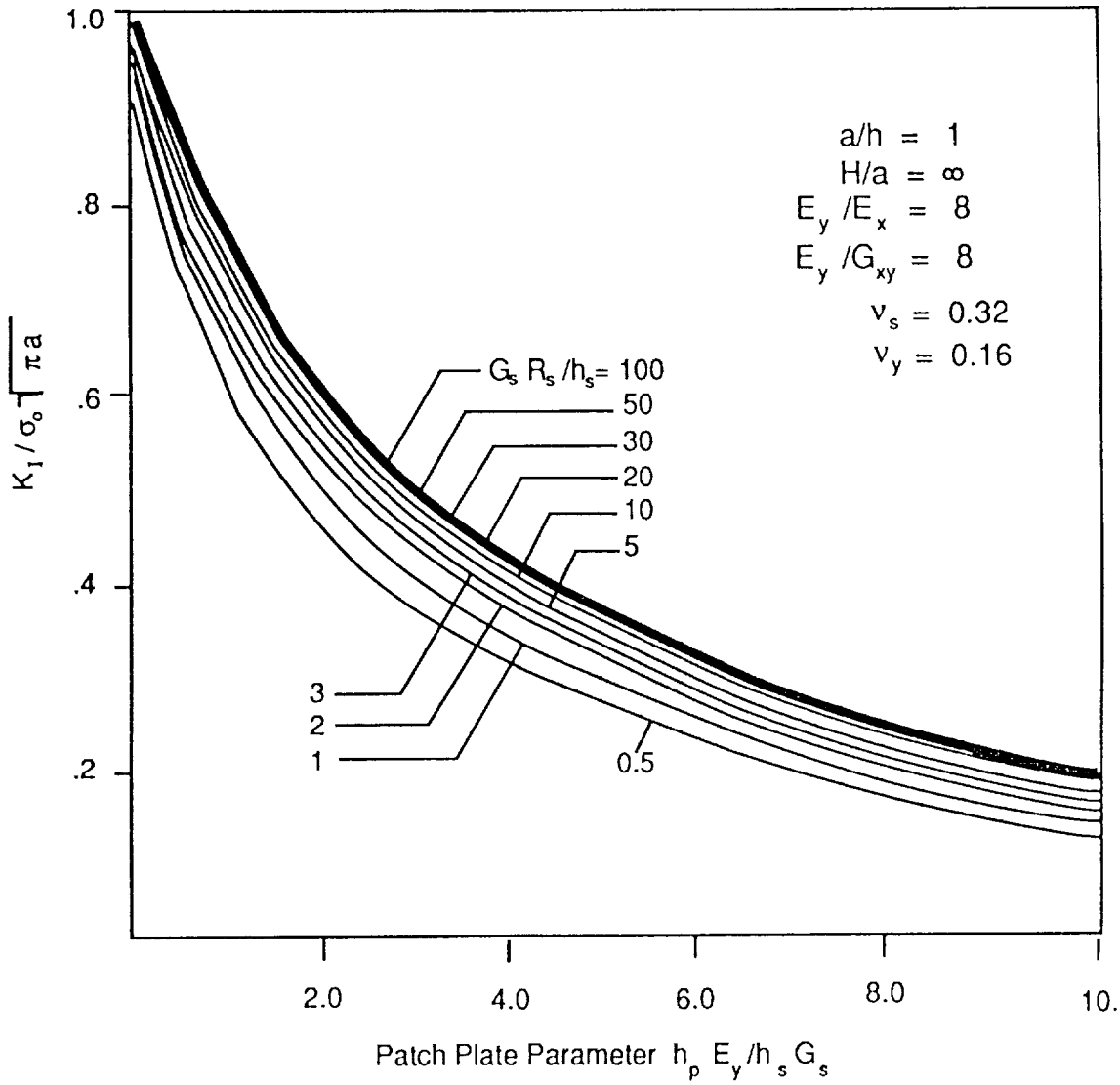

FIGURE 22 EFFECT OF PATCH PLATE ON THE STRESS INTENSITY FACTOR (FROM REFERENCE [37])

REFERENCES

1. "Proceedings of the International Conference on Aging Airplanes," DOT-TSC-FA890-88-26, June 1-3, 1988.

2. "Program Plan, National Aging Aircraft Research Program," Federal Aviation Administration, U.S. Department of Transportation, DOT-TSC-88-26, August, 1988.

3. "Proceedings of the Second International Conference on Aging Airplanes," Baltimore, DOT-FAA-CT-89-35, October, 1989.

4. Structural Integrity of Aging Airplanes, ed. by Atluri, S.N., Sampath, S.G. and Tong, P., Springer-Verlag, 1990.

5. Tong, P., "Multiple Site Damage," Proceedings of the Second International Conference on Aging Airplanes, Baltimore, October 1989.

6. Tong, P., Violette, M., and Sampath, S.G., "Research on MSD," DOT-VNTSC-FAID8-PP-90-2, Proceedings of Japan Society for Aeronautical and Space Sciences, 28th Aircraft Symposium, Tokyo, Japan, November 1990.

7. Tong, P., Sampath, S.C., and Broek, D., "Aging Aircraft, Detection of MSD, and the Risk of Failure," Paper presented at the ICAF Conference, Japan, 1991.

8. "Damage Tolerance Requirements FAR 25.571 and FAA AC 25.571.1," FAA Airworthiness Requirements, 1978.

9. "Airplane Damage Tolerance Requirements," Military Specification, MIL-A-83444 (USAF), 1974.

10. Samavedam, G. and Hoadley, D., "Fatigue and Fracture Strength Evaluation of Multiple Site Damage Aircraft Fuselages - Curved Panel Testing and Analysis," Foster-Miller, Inc., Waltham, MA, final report to Volpe National Transportation System Center, Contract DTRS-89-D-00009.

11. Pelloux, R.M. and Steul, D.R., "Failure Analysis Report, Foster-Miller Fatigue Test Panel," MIT report to VNTSC (April 23, 1991).

12. Swift, T., "Damage Tolerance in Pressurized Fuselage Structures," 11th Plantema Memorial Lecture, 14th Symposium of the International Committee on Aeronautical Fatigue, Ottawa, Canada, June 1987.

13. Swift, T., "Damage Tolerance Analysis of Redundant Structures," AGARD Lectures Series No. 97. Fracture Mechanics Design Methodology, 1979.

14. Mayville, R.A., and Warren, T. J., "A Laboratory Study of Fracture in the Presence of Lap Splice Multiple Site Damage," Structural Integrity of Aging Airplanes, ed. by Atluri, S.N., Sampath, S.G. and Tong, P., Springer-Verlag, 1990.

15. Hahn, G.J., and Shapiro, S.S., "A Catalog and Computer Program for the Design and Analysis of Orthogonal Symmetric and Asymmetric Fractional Factorial Experiments," General Electric Report No. 66-C-169, May 1966.

16. Tong, P., "A Hybrid Finite Element Method for Damage Tolerance Analysis," Computers and Structures, Vol. 19, No. 1-2, 263-269, 1984.

17. Pian, T.H.H. and Tong, P., "Basis of Finite Element Methods for Solid Continua," Int. J. Num. Meth. Eng., 1, pp. 3-28, 1969.

18. Tong, P., Pian, T.H.H. and Lasry, S.J., "A Hybrid Element Approach to Crack Problems in Plane Elasticity," Int. J. Num. Meth. Eng., Vol. 7, pp. 297-308, 1973.

19. Tong, P., Greif, R. and Chen, L., "Application of Hybrid Finite Element Method to Aircraft Repairs," 22th Conf. on Frac. Mech., Atlanta, Georgia, June 1990.

20. Tong, P., Greif, R. and Chen, L., "A Hybrid Finite Element Method for Damage Tolerance Analysis of Structures with Multiple Site Damage," Int. Conf. on Computational Eng. Sci., Melbourne, Australia, August 1991.

21. Standard E561-68, "Standard Practice for R-Curve Determination," Annual Book of Standards, Vol. 03.01, ASTM, Phila., PA, 1988.

22. Jeong, D.Y., Orringer, O. and Sih, G.C., "Strain Energy Density Approach to Stable Crack Extension under Net Section Yielding," Army Symposium on Solid Mechanics: Synergism of Mechanics, Mathematics, and Materials, Plymouth, MA, Nov. 4-7, 1991.

23. Jablonski, D.A., "Development of ACPD Procedures for Crack Detection in Aluminum Aircraft Panels," Instron Corporation, Canton, MA, final report to Volpe National Transportation Systems Center, Contract DTRS57-89-D-00007.

24. Pelloux, R.M., Warren, A., and O'Grady, J., "Fractographic Analysis of Initiation and Growth of Fatigue Cracks at Rivet Holes," Structural Integrity of Aging Airplanes, ed. by Atluri, S.N., Sampath, S.G. and Tong, P., Springer-Verlag, 1990.

25. Kobayashi, T., Shockey, D.A., and Giovanola, J.A., "Reconstruction of Fatigue Crack Behavior and Determination of Toughness Parameters from Fracture Surfaces," Structural Integrity of Aging Airplanes, ed. by Atluri, S.N., Sampath, S.G. and Tong, P., Springer-Verlag, 1990.

26. Broek, D., "The Feasibility of Proof Testing (a destructive inspection procedure)," published by FractuResearch Inc., TR 8916, September 1989.

27. Dawicke, D.S, Poe, C.C. Jr., Newman, J.C., Jr., and Harris, C.E., "An Evaluation of the Pressure Proof Test Concept for Thin Sheet 2024-T3," NASA TM-101675, National Aeronautics and Space Administration, 1990.

28. Harris, C.E. and Orringer, O., "Evaluation of the Concept of Pressure Proof Testing Fuselage Structures: Executive Summary," March, 1990.

29. Sampath, S. and Broek, D., "Estimation of Requirements of Inspection Intervals for Panels Susceptible to MSD," Structural Integrity of Aging Airplanes, ed. by Atluri, S.N., Sampth, S.G. and Tong, P., Springer-Verlag, 1990.

30. De Jonge J.B. et al, "A Standard Load Sequence for Flight-Simulation Testing," NLR-TR 73029, 1973.

31. Broek, D., The Practical Use of Fracture Mechanics, Kluwer, 1988.

32. Broek, D. and Kalev, L., "Inspection Intervals for Fixed Cumulative Probability of Detection," Paper presented at USAF-ASIP Conference, Dayton, 1985.

33. Broek, D., "Fracture Control by Periodic Inspection in Structure Failure, Product Liability and Technical Insurance," pp. 238-258, Interscience Enterprises, 1987.

34. Lincoln, J.W., "Risk Assessment of an Aging Military Aircraft," J. of Aircraft, Vol. 22, No. 8, pp. 687-691, 1985.

35. Orringer, O., "How Likely is Multiple Site Damage?" Structural Integrity of Aging Airplanes, ed. by Atluri, S.N., Sampath, S.G. and Tong, P., Springer-Verlag, 1990.

36. Swift, T., "Repairs to Damage Tolerant Aircraft," Structural Integrity of Aging Airplanes, edited by Atluri, S.N., Sampath, S.G., and Tong, P., Springer-Verlag, 1990.

37. Atluri, S.N., Knowledge Systems, Inc. Contractor Progress Reports, October 1990-October 1991.